

(12) INTERNATIONAL APPLICATION PUBLISHED UNDER THE PATENT COOPERATION TREATY (PCT)

(19) World Intellectual Property Organization  
International Bureau



(43) International Publication Date  
30 August 2001 (30.08.2001)

PCT

(10) International Publication Number  
**WO 01/62800 A1**

(51) International Patent Classification<sup>7</sup>: **C07K 16/18**, A61K 51/10, G01N 33/53, 33/574, 33/577, C07C 63/06, A61P 35/00

(21) International Application Number: PCT/EP01/02062

(22) International Filing Date: 23 February 2001 (23.02.2001)

(25) Filing Language: English

(26) Publication Language: English

(30) Priority Data:  
09/512,082 24 February 2000 (24.02.2000) US

(71) Applicant: **EIDGENÖSSISCHE TECHNISCHE HOCHSCHULE ZÜRICH [CH/CH]**; Rämistrasse 101, CH-8092 Zürich (CH).

(72) Inventors: **NERI, Dario**; Imbisbühlsteig 22, CH-8049 Zürich (CH). **TARLI, Lorenzo**; Via Abbadia, 20, I-53035 Monteriggioni (IT). **VITI, Francesca**; Via Battaglini, 16, I-16151 Genova (IT). **BIRCHLER, Manfred**; Anwandstrasse 66, CH-8004 Zürich (CH).

(74) Agent: **GERVASI, Gemma**; Notarbarloto & Gervasi S.P.A., Corso di Porta Vittoria, 9, I-20122 Milano (IT).

(81) Designated States (national): AE, AG, AL, AM, AT, AU, AZ, BA, BB, BG, BR, BY, BZ, CA, CH, CN, CR, CU, CZ, DE, DK, DM, DZ, EE, ES, FI, GB, GD, GE, GH, GM, HR, HU, ID, IL, IN, IS, JP, KE, KG, KP, KR, KZ, LC, LK, LR, LS, LT, LU, LV, MA, MD, MG, MK, MN, MW, MX, MZ, NO, NZ, PL, PT, RO, RU, SD, SE, SG, SI, SK, SL, TJ, TM, TR, TT, TZ, UA, UG, UZ, VN, YU, ZA, ZW.

(84) Designated States (regional): ARIPO patent (GH, GM, KE, LS, MW, MZ, SD, SL, SZ, TZ, UG, ZW), Eurasian patent (AM, AZ, BY, KG, KZ, MD, RU, TJ, TM), European patent (AT, BE, CH, CY, DE, DK, ES, FI, FR, GB, GR, IE, IT, LU, MC, NL, PT, SE, TR), OAPI patent (BF, BJ, CF, CG, CI, CM, GA, GN, GW, ML, MR, NE, SN, TD, TG).

Published:

- with international search report
- before the expiration of the time limit for amending the claims and to be republished in the event of receipt of amendments

For two-letter codes and other abbreviations, refer to the "Guidance Notes on Codes and Abbreviations" appearing at the beginning of each regular issue of the PCT Gazette.



**WO 01/62800 A1**

(54) Title: ANTIBODY SPECIFIC FOR THE ED-B DOMAIN OF FIBRONECTIN, CONJUGATES COMPRISING SAID ANTIBODY, AND THEIR USE FOR THE DETECTION AND TREATMENT OF ANGIOGENESIS

(57) Abstract: The present invention relates to antibodies with sub-nanomolar affinity specific for a characteristic epitope of the ED-B domain of fibronectin, a marker of angiogenesis. Furthermore, it relates to the use of radiolabelled high affinity anti ED-B antibodies for detecting new-forming blood vessels *in vivo* and a diagnostic kit comprising said antibody. Furthermore, it relates to conjugates comprising said antibodies and suitable photoactive molecules (e.g. an appropriately chosen photosensitizer or radionuclide), and their use for the selective light-mediated occlusion of new blood vessels.

1

ANTIBODY SPECIFIC FOR THE ED-B DOMAIN OF FIBRONECTIN, CONJUGATES COMPRISING SAID ANTIBODY, AND THEIR USE FOR THE DETECTION AND TREATMENT OF ANGIOGENESIS

Field of the Invention

5 The present invention relates to antibodies with sub-nanomolar affinity specific for a characteristic epitope of the ED-B domain of fibronectin, a marker of angiogenesis. It also relates to the use of radiolabelled high-affinity anti-ED-B antibodies for detecting new-forming blood vessels *in vivo* and a diagnostic kit comprising said antibody.

10 Moreover, the invention refers to conjugates comprising the above said antibodies and a suitable photoactive molecule (e.g., a photosensitizer) and to their use in the detection and/or coagulation of new blood vessels.

Background of the Invention

15 Tumours cannot grow beyond a certain mass without the formation of new blood vessels (angiogenesis), and a correlation between microvessel density and tumour invasiveness has been reported for a number of tumours (Folkman (1995). *Nature Med.*, 1, 27-31). Moreover, angiogenesis underlies the majority of ocular disorders which result in loss of vision [Lee et al., *Surv. Ophthalmol.* 43, 245-269 (1998); Friedlander, M. et al., *Proc. Natl. Acad. Sci. U.S.A.* 93, 9764-9769 (1996)].

20 Molecules capable of selectively targeting markers of angiogenesis would create clinical opportunities for the diagnosis and therapy of tumours and other diseases characterised by vascular proliferation, such as diabetic retinopathy and age-related macular degeneration. Markers of angiogenesis are expressed in the majority of aggressive solid tumours and should be readily accessible to specific binders injected intravenously (Pasqualini et al. (1997). *Nature Biotechnol.*, 15, 542-546; Neri et al. (1997), *Nature Biotechnol.*, 15 1271-1275). Targeted occlusion of the neovasculature may result in tumour infarction and collapse (O'Reilly et al. (1996). *Nature Med.*, 2, 689-692; Huang et al. (1997). *Science*, 275, 547-550).

25 The ED-B domain of fibronectin, a sequence of 91 aminoacids identical in mouse, rat and human, which is inserted by alternative splicing into the fibronectin molecule, specifically accumulates around neo-vascular structures (Castellani et al. (1994). *Int. J. Cancer* 59, 612-618) and could represent a target for molecular

intervention. Indeed, we have recently shown with fluorescent techniques that anti-ED-B single-chain Fv antibody fragments (scFv) accumulate selectively in tumoural blood vessels of tumour-bearing mice, and that antibody affinity appears to dictate targeting performance (Neri et al. (1997). *Nature Biotechnol.*, 15 1271-1275; International Patent Application No. PCT/GB97/01412, based on GB96/10967.3). Tumour targeting was evaluated 24 hours after injection, or at later time points.

Various attempts are known in the art to raise antibodies against the ED-B-domain in order to use them for tumour targeting.

10 Peters et al. (*Cell Adhesion and Communication* 1995, 3: 67-89) disclose polyclonal antibodies raised to antigens containing no FN sequence other than the intact ED-B domain and show that they bind specifically and directly to this domain.

15 However, the reagents of Peters et al. suffer from a series of drawbacks:- the antisera of Peters et al. recognise ED-B(+)-FN only after treatment with N-glycanase. This makes these reagents unsuitable for applications such as tumour targeting, imaging and therapy, as deglycosylation cannot be performed *in vivo*.

20 The authors acknowledge themselves that their antibodies do not recognise full-length ED-B(+)-FN produced by mammalian cells. They also acknowledge that it had been impossible to produce monoclonal antibodies specific for the ED-B domain of fibronectin, even though antibodies against other domains of fibronectin (such as ED-A) had been produced. It is well-known in the art that polyclonal antisera are unacceptable for above mentioned applications.

25 Even after years of intense research in this field, monoclonal antibodies recognising the ED-B domain of fibronectin without treatment with N-glycanase could be produced only using phage display techniques as applied in the present invention.

30 Zang et al. (*Matrix Biology* 1994, 14: 623-633) disclose a polyclonal antiserum raised against the canine ED-B domain. The authors do expect a cross-reactivity to human ED-B(+)-FN, although this was not tested. However, the authors acknowledge the difficulty to produce monoclonal antibodies directly recognising the ED-B domain of fibronectin (page 631). The antiserum recognises ED-B(+)-FN

in Western blot only after treatment with N-glycanase. As mentioned before, glycanase treatment renders these reagents unsuitable for applications according to the present invention.

Recognition of ED-B(+)-FN in ELISA proceeds without the need of deglycosylation  
5 but only on cartilage extracted with a denaturing agent (4M Urea) and captured on plastic using gelatin. The authors comment that "the binding of the FN molecule to the gelatine bound on the plastic surface of the ELISA plate may somehow expose the epitopes sufficiently for recognition by the antiserum". Since for *in vivo* applications FN cannot be denatured and gelatin bound, the monoclonal binders of  
10 the present invention offer distinct advantages.

The Japanese patents JP02076598 and JP04169195 refer to anti-ED-B antibodies. It is not clear from these documents if monoclonal anti ED-B antibodies are described. Moreover, it seems impossible that a single antibody (such as the antibody described in JP02076598) has "an antigen determinant in aminoacid  
15 sequence of formulae (1), (2) or (3):

- (1) EGIPIFEDFVDSSVGY
- (2) YTVTGLEPGIDYDIS
- (3) NGGESAPTTLTQQQT

on the basis of the following evidence:

20 i) A monoclonal antibody should recognise a well-defined epitope.  
ii) The three-dimensional structure of the ED-B domain of fibronectin has been determined by NMR spectroscopy. Segments (1), (2) and (3) lie on opposite faces of the ED-B structure, and cannot be bound simultaneously by one monoclonal antibody.  
25 Furthermore, in order to demonstrate the usefulness of the antibodies localisation in tumours should be demonstrated, as well as evidence of staining of ED-B(+)-FN structures in biological samples without treatment with structure-disrupting reagents.

The BC1 antibody described by Carnemolla et al. 1992, J. Biol. Chem. 267, 30 24689-24692, recognises an epitope on domain 7 of FN, but not on the ED-B domain, which is cryptic in the presence of the ED-B domain of fibronectin. It is strictly human-specific. Therefore, the BC1 antibody and the antibodies of the

present invention show different reactivity. Furthermore, the BC1 antibody recognises domain 7 alone, and domain 7-8 of fibronectin in the absence of the ED-B domain (Carnemolla et al. 1992, J. Biol. Chem. 267, 24689-24692). Such epitopes could be produced *in vivo* by proteolytic degradation of FN molecules.

5 The advantage of the reagents according to the present invention is that they can localise on FN molecules or fragments only if they contain the ED-B domain.

For the diagnosis of cancer, and more specifically for imaging primary and secondary tumour lesions, immunoscintigraphy is one of the techniques of choice. In this methodology, patients are imaged with a suitable device (e.g., a gamma 10 camera), after having been injected with radiolabelled compound (e.g., a radionuclide linked to a suitable vehicle). For scintigraphic applications, short-lived gamma emitters such as technetium-99m, iodine-123 or indium-111 are typically used, in order to minimise exposure of the patient to ionising radiations.

15 The most frequently used radionuclide in Nuclear Medicine Departments is technetium-99m (99mTc), a gamma emitter with half-life of six hours. Patients injected with 99mTc-based radiopharmaceuticals can typically be imaged up to 12-24 hours after injections; however, accumulation of the nuclide on the lesion of interest at earlier time points is desirable.

20 Furthermore, if antibodies capable of rapid and selective localisation on newly-formed blood vessels were available, researchers would be stimulated to search for other suitable molecules to conjugate to antibodies, in order to achieve diagnostic and/or therapeutic benefit.

#### Summary of the Invention

25 Considering the need of nuclear medicine for radiopharmaceuticals capable of localising tumour lesions few hours after injection, and the information that antibody affinity appears to influence its performance in targeting of angiogenesis, it is an object of the present invention to produce antibodies specific for the ED-B domain of fibronectin with sub-nanomolar dissociation constant (for a review on the definitions and measurements of antibody-antigen affinity, see Neri et al. 30 (1996). Trends in Biotechnol. 14, 465-470). A further object of the present invention is to provide radiolabelled antibodies in suitable format, directed against the ED-B domain of fibronectin, that detect tumour lesions already few hours after

injection.

In one aspect of the invention these objects are achieved by an antibody with specific affinity for a characteristic epitope of the ED-B domain of fibronectin and with improved affinity to said ED-B epitope.

5 In a further aspect of the present invention the above described antibody is used for rapid targeting markers of angiogenesis.

Another aspect of the present invention is a diagnostic kit comprising said antibody and one or more reagents for detecting angiogenesis.

10 Still a further aspect of the present invention is the use of said antibody for diagnosis and therapy of tumours and diseases which are characterized by vascular proliferation.

15 Finally, an important aspect of the invention is represented by conjugates comprising said antibodies and a suitable photoactive molecules (e.g. a judiciously chosen photosensitizer), and their use for the selective light-mediated occlusion of new blood vessels.

#### Terminology

Throughout the application several technical expressions are used for which the following definitions apply.

- antibody

20 This describes an immunoglobulin whether natural or partly or wholly synthetically produced. The term also covers any polypeptide or protein having a binding domain which is, or is homologous to, an antibody binding domain. These can be derived from natural sources, or they may be partly or wholly synthetically produced. Examples of antibodies are the immunoglobulin isotypes and their isotypic subclasses; fragments which comprise an antigen binding domain such as Fab, scFv, Fv, dAb, Fd; and diabodies. It is possible to take monoclonal and other antibodies and use techniques of recombinant DNA technology to produce other antibodies or chimeric molecules which retain the specificity of the original antibody. Such techniques may involve introducing DNA encoding the 25 immunoglobulin variable region, or the complementarity determining regions (CDRs), of an antibody to the constant regions, or constant regions plus framework regions, of a different immunoglobulin. See, for instance, EP-A-184187,

GB 2188638A or EP-A-239400. A hybridoma or other cell producing an antibody may be subject to genetic mutation or other changes, which may or may not alter the binding specificity of antibodies produced. As antibodies can be modified in a number of ways, the term "antibody" should be construed as covering any specific 5 binding member or substance having a binding domain with the required specificity. Thus, this term covers antibody fragments, derivatives, functional equivalents and homologues of antibodies, including any polypeptide comprising an immunoglobulin binding domain, whether natural or wholly or partially synthetic. Chimeric molecules comprising an immunoglobulin binding domain, or equivalent, 10 fused to another polypeptide are therefore included. Cloning and expression of chimeric antibodies are described in EP-A-0120694 and EP-A-0125023. It has been shown that fragments of a whole antibody can perform the function of binding antigens. Examples of binding fragments are (i) the Fab fragment consisting of VL, VH, CL and CH1 domains; (ii) the Fd fragment consisting of the 15 VH and CH1 domains; (iii) the Fv fragment consisting of the VL and VH domains of a single antibody; (iv) the dAb fragment (Ward et al. (1989) *Nature*, ), 341, 544-546.) which consists of a VH domain; (v) isolated CDR regions; (vi) F(ab')2 fragments, a bivalent fragment comprising two linked Fab fragments; (vii) single chain Fv molecules (scFv), wherein a VH domain and a VL domain are linked by a 20 polypeptide linker which allows the two domains to associate to form an antigen binding site (Bird et al. (1988) *Science*, 242, 423-426.; Huston et al. (1988) *Proc. Natl. Acad. Sci. U.S.A.*, 85, 5879-83.); (viii) bispecific single chain FV dimers (PCT/US92/09965) and (ix) "diabodies", multivalent or multispecific fragments 25 constructed by gene fusion (WO94/13804; Holliger et al. (1993) *Proc. Natl. Acad. Sci. U.S.A.*, 90, 6444-6448). Diabodies are multimers of polypeptides, each polypeptide comprising a first domain comprising a binding region of an immunoglobulin light chain and a second domain comprising a binding region of an immunoglobulin heavy chain, the two domains being linked (e.g. by a peptide linker) but unable to associate with each other to form an antigen binding site: 30 antigen binding sites are formed by the association of the first domain of one polypeptide within the multimer with the second domain of another polypeptide within the multimer (WO94/13804). Where bispecific antibodies are to be used,

these may be conventional bispecific antibodies, which can be manufactured in a variety of ways Holliger and Winter (1993), Curr. Opin. Biotech., 4, 446-449), e.g. prepared chemically or from hybrid hybridomas, or may be any of the bispecific antibody fragments mentioned above. It may be preferable to use scFv dimers or 5 diabodies rather than whole antibodies. Diabodies and scFv can be constructed without an Fc region, using only variable domains, potentially reducing the effects of anti-idiotypic reaction. Other forms of bispecific antibodies include the single-chain CRAbs described by Neri et al. ((1995) J. Mol. Biol., 246, 367-373).

- complementarity-determining regions
- 10 Traditionally, complementarity-determining regions (CDRs) of antibody variable domains have been identified as those hypervariable antibody sequences, containing residues essential for specific antigen recognition. In this document, we refer to the CDR definition and numbering of Chothia and Lesk (1987) J. Mol. Biol., 196, 901-917.

- 15 - functionally equivalent variant form

This refers to a molecule (the variant) which although having structural differences to another molecule (the parent) retains some significant homology and also at least some of the biological function of the parent molecule, e.g. the ability to bind a particular antigen or epitope. Variants may be in the form of fragments, 20 derivatives or mutants. A variant, derivative or mutant may be obtained by modification of the parent molecule by the addition, deletion, substitution or insertion of one or more aminoacids, or by the linkage of another molecule. These changes may be made at the nucleotide or protein level. For example, the encoded polypeptide may be a Fab fragment which is then linked to an Fc tail from another source. Alternatively, a marker such as an enzyme, fluorescein, etc, may 25 be linked. For example, a functionally equivalent variant form of an antibody "A" against a characteristic epitope of the ED-B domain of fibronectin could be an antibody "B" with different sequence of the complementarity determining regions, but recognising the same epitope of antibody "A".

- 30 We have isolated recombinant antibodies in scFv format from an antibody phage display library, specific for the ED-B domain of fibronectin, and recognising ED-B(+)-fibronectin in tissue sections. One of these antibodies, E1, has been affinity

matured to produce antibodies H10 and L19, with improved affinity. Antibody L19 has a dissociation constant for the ED-B domain of fibronectin in the sub-nanomolar concentration range.

The high-affinity antibody L19 and D1.3 (an antibody specific for an irrelevant antigen, hen egg lysozyme) were radiolabelled and injected in tumour-bearing mice. Tumour, blood and organ biodistributions were obtained at different time points, and expressed as percent of the injected dose per gram of tissue (%ID/g). Already 3 hours after injection, the %ID/g (tumour) was better than the %ID/g (blood) for L19, but not for the negative control D1.3. The tumour : blood ratios increased at longer time points. This suggests that the high-affinity antibody L19 may be a useful tumour targeting agent, for example for immunoscintigraphic detection of angiogenesis.

- photosensitizer (or photosensitiser)

A photosensitiser could be defined as a molecule which, upon irradiation and in the presence of water and/or oxygen, will generate toxic molecular species (e.g., singlet oxygen) capable of reacting with biomolecules, therefore potentially causing damage to biological targets such as cells, tissues and body fluids.

Photosensitisers are particularly useful when they absorb at wavelengths above 600 nm. In fact, light penetration in tissues and body fluids is maximal in the 600 – 900 nm range [Wan et al. (1981) *Photochem. Photobiol.* 34, 679-681].

The targeted delivery of photosensitisers followed by irradiation is an attractive avenue for the therapy of angiogenesis-related diseases [Yarmush, M.L. et al. Antibody targeted photolysis. *Crit. Rev. Therap. Drug Carrier Systems* 10, 197-252 (1993); Rowe, P.M. *Lancet* 351, 1496 (1998); Levy, J. *Trends Biotechnol.* 13, 14-18 (1995)), particularly for the selective ablation of ocular neovasculature. Available therapeutic modalities such as laser photocoagulation, either directly or after administration of photosensitising agents, are limited by a lack of selectivity and typically result in the damage of healthy tissues and vessels [Macular Photocoagulation Study Group, *Arch. Ophtalm.* 112, 480-488 (1994); Haimovici, R. et al., *Curr. Eye Res.* 16, 83-90 (1997); Schmidt-Erfurth, U. et al.; *Graefes Arch. Clin. Exp. Ophthalmol.* 236, 365-374 (1998).].

On the basis of the arguments presented above, one can see that it would be

extremely important to discover ways to improve the selectivity and specificity of photosensitisers, for example by conjugating them to a suitable carrier molecule. It is likely that the development of good-quality carrier molecules will not be a trivial task. Moreover, it is likely that not all photosensitisers will lend themselves to be „vehicled“ in vivo to the site of interest. Factors such as photosensitiser chemical structure, solubility, lipophilicity, stickiness and potency are likely to crucially influence the „targetability“ and efficacy of photosensitisers' conjugates.

Here we show that the high-affinity L19 antibody, specific for the ED-B domain of fibronectin selectively localises to newly formed blood vessels in a rabbit model of 10 ocular angiogenesis upon systemic administration. The L19 antibody, chemically coupled to the photosensitising agent tin (IV) chlorin e<sub>6</sub> and irradiated with red light, mediated the selective occlusion of ocular neovasculature and promoted apoptosis of the corresponding endothelial cells. These results demonstrate that new ocular blood vessels can be distinguished immunochemically from pre-existing ones in vivo, and strongly suggest that targeted delivery of 15 photosensitisers followed by irradiation may be effective in treating blinding eye diseases and possibly other pathologies associated with angiogenesis.

Another important feature to be considered when conjugates containing a 20 photosensitisers are used is the fact that photosensitisers are among the few species capable of mediating their toxic activity in the immediate proximity of the antibody to which they have been conjugated.

Upon irradiation and in the presence of oxygen, most photosensitisers produce, among other reactive species, singlet oxygen: a diffusive toxic molecule capable of 25 damaging cells by reacting with membranes, proteins and DNA. The average diffusion of singlet oxygen has been estimated to be around 200 nm (Yarmush et al. 1993, Crit. Rev. Ther. Drug, 10, 197-252).

The same applies to alpha-emitting radionuclides, such as astatine-211, bismuth-212 and bismuth-213, which produce energetic alpha particles having a range in tissue penetration of 50-100  $\mu$ M (Hauck et al. 1998, Brit. J. Cancer 77, 753-759), 30 depositing energy that is about 500 times greater than that of beta particles, e.g. yttrium-90 (100 KeV/ $\mu$ M vs. 0.2 KeV/ $\mu$ M, respectively) (McDevitt et al. 1998, Eur. J. Nucl. Med. 25, 1341-135).

Photosensitisers or alpha-emitting radionuclides conjugated to the antibodies specific for the ED-B domain of fibronectin described in the present application, as for example L 19, can be targeted to new blood vessels *in vivo*, as illustrated in the examples hereinafter reported. Thanks to this exquisite specificity of localisation and to the short range of action of the toxic species released by photosensitiser and alpha-emitting radionuclides, specific damage can be inferred in the immediate proximity of the labelled antibody, while sparing adjacent tissues/cells.

Toxic species with a short path of action (such as singlet oxygen and alpha particles), when delivered by the L19 antibody, offer the possibility to selectively damage the endothelial cells of new blood vessels, while sparing normal tissues and blood cells. This level of selectivity should offer tremendous advantages for the control of angiogenesis-related disorders, such as cancer, rheumatoid arthritis, neo-vasculature associated ocular disorders and psoriasis.

The innovative concept of delivering short-range acting toxic agents to new blood vessels, while sparing established blood vessels and normal tissues, can be easily appreciated in the light of the following considerations.

Let us consider the biodistribution studies performed in tumour-bearing mice injected with radiolabelled L19, described in Example 3. When using the L19 antibody labelled with a beta-particle emitting radionuclide (e.g., Yttrium-90), the antibody delivers beta particles to the neighbouring cells/tissues with a penetration of several millimetres. Let us assume that all tissues in the body are equally radiosensitive, let us neglect radioactive decay, and let us remember that radioactivity will begin to exhibit its biocidal effect from the moment the radiolabelled antibody is injected intravenously (i.e., from time = 0 s). The therapeutic advantage of the radiolabelled antibody will be related to the ratio between the total dose of radioactivity delivered by the antibody to the tumour and the total dose of radioactivity delivered by the antibody to blood or organs, normalised per gram of fluid or tissue (Behr et al. 1998, Int. J. Cancer 77, 787-795).

Let us examine the biocidal dose delivered to the tumour and to blood (representative of myelotoxicity, which is typically the limiting toxicity with radiolabelled antibodies).

The dose of radioactivity delivered per gram of tumour is proportional to the area under the curve (AUC) of the %ID/g (tumour), plotted versus time. Analogously, the dose of radioactivity delivered to blood is proportional to the area under the curve (AUC) of the %ID/g (blood), plotted versus time. During the first 24 hours 5 after intravenous injection the ratio of AUC(tumour) / AUC(blood) is equal to 3.6 (Figure 13). This ratio may somewhat increase when the AUCs are measured for longer time periods, but therapeutic ratios greater than 6-7 are rarely achieved. Let us now consider the situation in which a short-range-acting toxic species (e.g., 10 a photosensitiser or an alpha-particle emitting radionuclide) is delivered to the tumoural blood vessels, and is therefore not homogenously distributed in the tumour mass. The diffusive toxic species (e.g., singlet oxygen or an alpha particle) will hardly penetrate more than one layer of cells, i.e. will hit only the endothelial 15 cells lining the tumour blood vessel wall. Since new-forming blood vessels in most tumours (including the F9 teratocarcinoma) constitute less than 2% of the total tumour mass, the relevant parameter for predicting therapeutic benefit will be the 20 ratio AUC(vessel) / AUC(blood).

As we can see in Figure 14, L19 accumulates only around new blood vessels. This 25 observation has also been confirmed by microautoradiographic analysis in tumours (Tarli et al. 1999, Blood, 94, 192-198). Since the radioactivity delivered to tumours is concentrated around neo-vascular structures, and assuming that tumoural vasculature accounts for 2% of the tumour weight, we can calculate that AUC(vessel) = (100/2) x AUC(tumour) = 50 x AUC(tumour). In other words, the 30 selectivity of the treatment is expected to be proportional to the ratio AUC(vessel) / AUC(blood), which is > 150:1 over a period of 24 hours in our experimental system (see also Figure 15 for explanation).

Let us consider astatine-211 as a particularly interesting alpha-particle emitting 35 radionuclide for biomedical application. The half-life of its radioactive decay is considerably longer than the ones of bismuth-212 and bismuth-213 (7.2 hrs, compared to 1.0 hr and 45 min., respectively) (Larsen and Bruland 1998, Brit. J. Cancer 77, 1115-1122). Astatine is the heaviest halogen and no stable isotopes of this element exist. Since it is directly below iodine in the periodic table, it might be 40 expected that the two halogens would possess similar chemical properties.

However, attempts to label proteins with  $^{211}\text{At}$  by direct electrophilic astatination at the level of the protein aminoacid did not give successful results because of rapid loss of label following *in vivo* administration (Vaughan et al. 1978, Int. J. Nucl. Med. 5, 229-230). To circumvent this problem, L19 can be conjugated with  $^{211}\text{At}$  with significant nuclide incorporation and no loss of antibody specificity by the two-step labeling method published by Garg (Garg et al. 1989, Appl. Radiat. Isot. 40, 485-490). It involves the use of a bifunctional chemical compound, N-succinimidyl-3-(trimethylstannyl)-benzoate (m-MeATE; ATE, «alkyltin ester») (Zalutsky et al. 1989, Proc. Natl. Acad. Sci. USA 86, 7149-7153), which we synthesized following the protocol published by Garg (see Figure 16) as reported in Example 7.

It is important to report that using equimolar amount of m-bromobenzoic acid and trimethylstannyl-chloride, the reaction product is 3-(trimethylstannyl)benzoic acid rather than the published trimethylstannyl-3-(trimethylstannyl) benzoate. Based on the results of the labeling experiments, described below, we believe that this compound may have superior qualities compared to the previously described trimethylstannyl-3-(trimethylstannyl) benzoate derivatives.

The bifunctional m-MeATE agent can be used both to label L19 with the gamma-emitting iodine-125 and the alpha-emitting astatine-211 in a two-step methodology. Protein labeling with iodine-125 through m-MeATE rather than conventional electrophilic methods (e.g. the chloramine-T and the Iodogen methods) is reported to provide protein iodination sites which are more inert towards dehalogenation *in vivo* (Garg et al. 1989, Appl. Radiat. Isot. 40, 485-490). The labeling protein coupling efficiency together with the conjugate immunoreactivity arising from this two-step radiolabeling methodology were studied through the reaction with iodine-125.

In the first step, m-MeATE and t-butylhydroperoxide (TBHP) were added to  $\text{Na}^{125}\text{I}$ . Following a 20 minutes incubation period, the radioiodinated product N-succinimidyl-3-( $^{125}\text{I}$ )-benzoate was isolated and separated from unconjugated m-MeATE by chromatography using a disposable silica gel Sep-Pak column and a gradient of ethyl acetate in hexane as eluent phase. Starting from 100  $\mu\text{Ci}$  of  $\text{Na}^{125}\text{I}$ , we coupled 90  $\mu\text{Ci}$  of  $^{125}\text{I}$  to the N-succinimidyl benzoate. A solution of L19 in borate buffer (pH = 8.5) was added in the second step to the purified N-

succinimidyl-3-(<sup>125</sup>I)-benzoate. Following an incubation time of 30 minutes on ice, the radiolabelled L19 was separated from unincorporated iodine using a PD-10 disposable gel filtration column. The resulting efficiency of L19 labeling using radioiodinated ATE resulted to be strongly dependent on initial protein concentration. Using L19 at a concentration of 0.42 µg/µl and 1 µg/µl, 18% and 28% of starting radiolabelled benzoate was coupled to L19, respectively. According to these results, if we started from 1 mCi of Na<sup>125</sup>I and a concentration of L19 of 1 µg/µl, we would obtain L19 labelled with <sup>125</sup>I at a specific activity of 1 µCi/µl. The initial concentration of L19 did not influence the immunoreactivity of the conjugates after labeling. Following the method reported in example 3, the immunoreactivity, defined as reported by Viti et al. (Viti et al. 1999, Cancer Research 59, 347-352) resulted to be in both cases > 90%.

These results demonstrate the feasibility of the labeling of L19 with radiohalogens using the bifunctional m-MeATE.

Astatine-211 may offer the additional advantage that it is likely to be detached from L19 by dehalogenases in the kidney glomeruli (T. M. Behr et al. 1999, Cancer Res. 59, 2635-43), but not in tumoural vessels, therefore reducing kidney toxicity of the radiolabelled compound in spite of the clearance of the immunoconjugate via the renal route. For photosensitisers, glomeruli in the kidneys will not be damaged, since for most applications irradiation of the kidneys is not foreseen.

It is obviously also possible to prepare conjugates consisting of the antibody linked to a photosensitiser and a radionucleide in order to take advantages of the activity of both.

Brief Description of the Drawings

Embodiments of the present invention are illustrated by the following figures, wherein

- Fig. 1 shows a designed antibody phage library;
- Fig. 2 shows 2D gels and Western blotting of a lysate of human melanoma COLO-38 cells;
- Fig. 3 shows immunohistochemical experiments of glioblastoma multiforme
- Fig. 4 shows an analysis of the stability of antibody-(ED-B) complexes.
- Fig. 5 shows biodistribution of tumour bearing mice injected with radiolabelled

antibody fragments.

Fig. 6 shows amino acid sequence of L19;

Figure 7 shows rabbit eyes with implanted pellet;

Figure 8 shows immunohistochemistry of rabbit cornea sections.

5 Figure 9 shows the immunohistochemistry of sections of ocular structures of rabbits (cornea, iris and conjunctiva) using a red alkaline phosphatase substrate and hematoxylin.

Figure 10 shows the localisation of fluorescently-labelled antibodies in ocular neovasculature.

10 Figure 11 shows the macroscopic appearance of the eyes of rabbits injected with proteins coupled to photosensitizers, before and after irradiation.

Figure 12 shows the microscopic analysis of sections of ocular structures of rabbits injected with proteins coupled to photosensitizers and irradiated with red light.

15 Figure 13 shows schematic diagrams in which the % of injected dose delivered per gram, respectively of blood and tumour, are plotted versus time.

Figure 14 shows the accumulation of L19 around new vessels.

Figure 15 shows schematic diagrams reporting the relevant % of injected doses per gram, in the case of the L19 antibody coupled to an  $\alpha$ - and  $\beta$ -emitter 20 respectively, plotted versus time.

Figure 16 shows the labelling method according to the Garg protocol modified as described hereinafter.

Figures 17a and 17b report the  $^1\text{H-NMR}$  spectrum of 3-(trimethylstannyl)-benzoic acid.

25 Figures 18 a and 18b report the  $^1\text{H-NMR}$  spectrum of N-succinimidyl-3-(trimethylstannyl)-benzoate

Figure 19 shows the EI-MS of N-succinimidyl-3-(trimethylstannyl)-benzoate.

#### Detailed Description of the Drawings

Figure 1 shows:

30 Designed antibody phage library. (a) Antibody fragments are displayed on phage as pIII fusion, as schematically depicted. In the antibody binding site (antigen's eye view), the  $\text{V}_\text{L}$  CDRs backbone is in yellow, the  $\text{V}_\text{H}$  CDR backbone is in blue.

Residues subject to random mutation are Vk CDR3 positions 91, 93, 94 and 96 (yellow), and VH CDR3 positions 95, 96, 97, and 98 (blue). The Cb atoms of these side chains are shown in darker colours. Also shown (in grey), are the residues of CDR1 and CDR2, which can be mutated to improve antibody affinity. Using the 5 program RasMol (<http://www.chemistry.ucsc.edu/wipke/teaching/rasmol.html>), the structure of the scFv were modeled from pdb file 1igm (Brookhaven Protein Data Bank; <http://www2.ebi.ac.uk/pcserv/pdbdb.htm>). (b) PCR amplification and library cloning strategy. The DP47 and DPK22 germline templates were modified (see text) to generate mutations in the CDR3 regions. Genes are indicated as 10 rectangles, and CDRs as numbered boxes within the rectangle. The VH and the VL segments were then assembled and cloned in pDN332 phagemid vector. Primers used in the amplification and assembly are listed at the bottom.

Figure 2 shows

2D gels and western blotting (a) Silver-staining of the 2D-PAGE of a lysate of 15 human melanoma COLO-38 cells, to which recombinant ED-B-containing 7B89 had been added. The two 7B89 spots (circle) are due to partial proteolysis of the His-tag used for protein purification. (b) Immunoblot of a gel, identical to the one of Fig. 2a, using the anti-ED-B E1 (Table 1) and the M2 anti-FLAG antibodies as 20 detecting reagent. Only the 7B89 spots are detected, confirming the specificity of the recombinant antibody isolated from a gel spot.

Figure 3 shows:

Immunohistochemical experiments on serial sections of glioblastoma multiforme showing the typical glomerulus-like vascular structures stained using scFvs E1 (A), A2 (B) and G4 (C). Scale bars: 20  $\mu$ m.

25 Figure 4 shows:

Stability of antibody-(ED-B) complexes. Analysis of the binding of scFvs E1, H10 and L19 to the ED-B domain of fibronectin. (a) BIACore sensograms, showing the improved dissociation profiles obtained upon antibody affinity-maturation. (b) Native gel electrophoretic analysis of scFv-(ED-B) complexes. Only the high-affinity antibody L19 can form a stable complex with the fluorescently labelled 30 antigen. Fluorescence detection was performed as described (Neri et al. (1996) BioTechniques, 20, 708-712).

(c) Competition of the scFv-(ED-B-biotin) complex with a 100-fold molar excess of unbiotinylated ED-B, monitored by electrochemiluminescence using an Origen apparatus. A long half-life for the L19-(ED-B) complex can be observed. Black squares: L19; Open triangles: H10.

5 Figure 5 shows:

Biodistributions of tumour bearing mice injected with radiolabelled antibody fragments.

Tumour and blood biodistributions, expressed as percent injected dose per gram, are plotted versus time. Relevant organ biodistributions is also reported.

10 Figure 6 shows the amino acid sequence of antibody L19 comprising the heavy chain (VH), the linker and the light chain (VL).

Figure 7 shows rabbit eyes with implanted polymer pellets soaked with angiogenic substances.

15 Figure 8 shows immunohistochemistry of sections of rabbit cornea with new-forming blood vessels, stained with the L19 antibody.

Figure 9 shows immunohistochemical studies of ocular structures using the L19 antibody. A specific red staining is observed around neovascular structures in the cornea (a), but not around blood vessels in the iris (b) and in the conjunctiva (c). Small arrows: corneal epithelium. Relevant blood vessels are indicated with large 20 arrows. Scale bars: 50 µm

Figure 10 shows immunophotodetection of fluorescently labelled antibodies targeting ocular angiogenesis. A strongly fluorescent corneal neovascularisation (indicated by an arrow) is observed in rabbits injected with the antibody conjugate L19-Cy5 (a), specific for the ED-B domain of FN, but not with the antibody HyHEL-25 10-Cy5 (b). Immunofluorescence microscopy on cornea sections confirmed that L19-Cy5 (c), but not HyHEL-10-Cy5 (d) localises around neovascular structures in the cornea. Images (a,b) were acquired 8 h after antibody injection; (c, d) were obtained using cornea sections isolated from rabbits 24 h after antibody injection.

P, pellet.

30 Figure 11 shows macroscopic images of eyes of rabbits treated with photosensitiser conjugates. Eye of rabbit injected with L19-PS before (a) and 16 h after irradiation with red light (b). The arrow indicates coagulated neovasculature,

which is confirmed as a hypofluorescent area in the Cy5 fluoroangiogram of panel (c) 16 h after irradiation. Note that no coagulation is observed in other vascular structures, for example in the dilated conjunctival vessels. For comparison, a Cy5 fluoroangiogram with hyperfluorescence of leaky vessels, and the corresponding 5 colour photograph of untreated rabbit eye are shown in (d) and (h). Pictures (e,f,g) are analogous to (a,b,c), but correspond to a rabbit injected with ovalbumin-PS and irradiated with red light. No coagulation can be observed, and the angiogram reveals hyperfluorescence of leaky vessels. The eyes of rabbits with early-stage 10 angiogenesis and injected with L19-PS are shown in (i-l). Images before (i) and 16 h after irradiation with red light (j) reveal extensive and selective light-induced 15 intravascular coagulation (arrow). Vessel occlusion (arrow) is particularly evident in the irradiated eye (l) of a rabbit immediately after euthanasia, but cannot be detected in the non-irradiated eye (k) of the same rabbit. P, pellet. Arrowheads indicate the corneo-scleral junction (limbus). In all figures, dilated pre-existing conjunctival vessels are visible above the limbus, whereas growth of corneal neovascularisation can be observed from the limbus towards the pellet (P).

Figure 12 shows microscopic analysis of selective blood vessel occlusion. H/E sections of corneas (a,e,b,f: non-fixed; i,j: paraformaldehyde fixed) of rabbits injected with ovalbumin-PS (a,e,i) or L19-PS (b,f,j) and irradiated. Large arrows 20 indicate representative non damaged (e,i) or completely occluded (f,j) blood vessels. In contrast to the selective occlusion of corneal neovasculature and restricted perivascular damage (eosinophilia) mediated by L19-PS after irradiation (b,f,j), vessels in the conjunctiva (k) and iris (l) do not show sign of damage in the same rabbit. Fluorescent TUNEL assay indicates the different number of apoptotic 25 cells in sections of irradiated rabbits injected with L19-PS (c,g) or with ovalbumin-PS (d,h). Large arrows indicate some relevant vascular structures. Small arrows indicate corneal epithelium. Scale bars: 100 µm (a-d) and 25 µm (e-l)

Figure 13 shows the area under the curve (AUC) of the radioactivity delivered by scFv(L19) to the blood and to the tumour during the first 24 hours after intravenous 30 injection. In this experimental study performed in mice bearing the F9 teratocarcinoma, the AUC of the injected dose of radiolabelled antibody delivered

per gram of tumour is 3.6-fold higher than the dose delivered per gram of blood. This ratio increases when the AUC is measured for longer time periods.

Figure 14 shows microautoradiographic analysis of an F9 teratocarcinoma dissected from a nude mouse, after injection of radiolabelled scFv(L19). The 5 pictures show that scFv(L19) accumulates around vascular structure but not in the surrounding normal mouse tissue.

Figure 15 illustrates a schematic diagram of the radiimmunotherapy performed with the anti-angiogenesis scFv(L19) coupled with  $\beta$ - or  $\alpha$ -emitting radionuclide. Because new-forming blood vessels in F9 teratocarcinoma constitute 0.5-5% of

10 the total tumour mass, the radioactivity delivered to vascular structures is significantly higher (70-700-fold) than the one delivered to normal tissue and to blood. Coupling scFv(L19) to a beta emitter (e.g., Yttrium-90), the majority of the 15 targeted tumoural area is irradiated, since these  $\beta$ -particles have a range in tissue of several millimiters. On the other hand, coupling scFv(L19) to an alpha emitter (e.g. Astatine-211 or Bismuth-212 or Bismuth-213), the radiation is deposited only around the targeted tumoural blood vessels (penetration: few dozens of micrometers). In this case, the relevant parameters for therapeutic efficacy is the vessel:blood ratio of the percent injected dose of radioactivity per gram of tissue, rather than the tumour:blood ratio (which is the relevant parameter for beta 20 emitting nuclides).

Figure 16 shows the procedure for labelling scFv(L19) with Iodine-125 and Astatine-211 using the N-succinimidyl 3-(trimethylstannyl)benzoate (m-MeATE) synthesized from m-bromobenzoic acid.

Figure 17A shows the  $^1\text{H}$ -NMR spectrum of 3-(trimethylstannyl)benzoic acid in  $\text{CDCl}_3$ . The chemical shifts (ppm) are indicated in the X-axis.

Figure 17B shows the chemical shift in ppm of the protons in the aromatic moiety located at low magnetic field of the NMR spectrum.

Figure 18A shows the  $^1\text{H}$ -NMR spectrum of m-MeATE in  $\text{CDCl}_3$ . The relative values of peak intensity are reported between the X-axis reporting the chemical 30 shift (ppm) and the spectrum baseline.

Figure 18B shows an enlarged portion of the  $^1\text{H}$ -NMR spectrum of m-MeATE.

Figure 19 shows the electron ionization mass spectrum (EI-MS) of m-MeATE (molecular weight 383). The mass to charge value (m/e) of 368 represents the mass of the molecular ion ( $M^+$ ) - 15 ( $CH_3$ ).

The invention is more closely described by the following examples.

5 Example 1

Isolation of human scFv antibody fragments specific for the ED-B domain of fibronectin from a antibody phage-display library

A human antibody library was cloned using VH (DP47; Tomlinson et al. (1992). J. Mol. Biol., 227, 776-798.) and Vk (DPK22; Cox et al. (1994). Eur. J. Immunol., 24, 10 827-836) germline genes (see Figure 1 for the cloning and amplification strategy). The VH component of the library was created using partially degenerated primers (Figure 1) in a PCR-based method to introduce random mutations at positions 95-98 in CDR3. The VL component of the library was generated in the same manner, by the introduction of random mutations at positions 91, 93, 94 and 96 of CDR3. 15 PCR reactions were performed as described (Marks et al. (1991). J. Mol. Biol., 222, 581-597). VH-VL scFv fragments were constructed by PCR assembly (Figure 1; Clackson et al. (1991). Nature, 352, 624-628), from gel-purified VH and VL segments. 30 $\mu$ g of purified VH-VL scFv fragments were double digested with 300 units each of NcoI and NotI, then ligated into 15  $\mu$ g of NotI/NcoI digested pDN332 20 phagemid vector. pDN332 is a derivative of phagemid pHEN1 (Hoogenboom et al. (1991). Nucl. Acids Res., 19, 4133-4137), in which the sequence between the NotI site and the amber codon preceding the gene III has been replaced by the following sequence, coding for the D3SD3-FLAG-His6 tag (Neri et al. (1996). Nature Biotechnology, 14, 385-390):

25

NotI D D D S D D D  
Y K D D  
5' - GCG GCC GCA GAT GAC GAT TCC GAC GAT GAC TAC AAG GAC GAC

30

D D K H H H H H amber  
GAC GAC AAG CAC CAT CAC CAT CAC CAT TAG - 3'

Transformations into TG1 E.coli strain were performed according to Marks et al. (1991. J. Mol. Biol., 222, 581-597) and phages were prepared according to

standard protocols (Nissim et al. (1991). *J. Mol. Biol.*, 222, 581-597). Five clones were selected at random and sequenced to check for the absence of pervasive contamination.

Recombinant fibronectin fragments ED-B and 7B89, containing one and four type III homology repeats respectively, were expressed from pQE12-based expression vectors (Qiagen, Chatsworth, CA, USA) as described (Carnemolla et al. (1996). *Int. J. Cancer*, 68, 397-405).

Selections against recombinant ED-B domain of fibronectin (Carnemolla et al. (1996). *Int. J. Cancer*, 68, 397-405, Zardi et al. (1987). *EMBO J.*, 6, 2337-2342)

were performed at 10 nM concentration using the antigen biotinylated with biotin disulfide N-hydroxysuccinimide ester (reagent B-4531; Sigma, Buchs, Switzerland; 10) and eluted from a 2D gel, and streptavidin-coated Dynabeads capture (Dynal, Oslo, Norway). 1013 phages were used for each round of panning, in 1 ml reaction. Phages were incubated with antigen in 2% milk/PBS (MPBS) for 10 minutes. To this solution, 100 µl Dynabeads (10 mg/ml; Dynal, Oslo, Norway), preblocked in MPBS, were added. After 5 min. mixing, the beads were magnetically separated from solution and washed seven times with PBS-0.1% Tween-20 (PBST) and three times with PBS. Elution was carried out by incubation for 2 min. with 500 µl 50 mM dithiothreitol (DTT), to reduce the disulfide bridge 15 between antigen and biotin. Beads were captured again, and the resulting solution 20 was used to infect exponentially growing TG1 *E.coli* cells. After three rounds of panning, the eluted phage was used to infect exponentially-growing HB2151 *E.coli* cells and plated on (2xTY + 1% glucose + 100 µg/ml ampicillin) - 1.5% agar plates. Single colonies were grown in 2xTY + 0.1% glucose + 100 µg/ml ampicillin, and 25 induced overnight at 30 degrees with 1 mM IPTG to achieve antibody expression.

The resulting supernatants were screened by ELISA using streptavidin-coated microtitre plates treated with 10 nM biotinylated-ED-B, and anti-FLAG M2 antibody (IBI Kodak, New Haven, CT) as detecting reagent. 32% of screened clones were positive in this assay and the three of them which gave the strongest ELISA signal 30 (E1, A2 and G4) were sequenced and further characterised.

ELISA assays were performed using biotinylated ED-B recovered from a gel spot, biotinylated ED-B that had not been denatured, ED-B linked to adjacent fibronectin

domains (recombinant protein containing the 7B89 domains), and a number of irrelevant antigens. Antibodies E1, A2 and G4 reacted strongly and specifically with all three ED-B containing proteins. This, together with the fact that the three recombinant antibodies could be purified from bacterial supernatants using an ED-B affinity column, strongly suggests that they recognise an epitope present in the native conformation of ED-B. No reaction was detected with fibronectin fragments which did not contain the ED-B domain (data not shown).

In order to test whether the antibodies isolated against a gel spot had a good affinity towards the native antigen, real-time interaction analysis was performed using surface plasmon resonance on a BIAcore instrument as described (Neri et al. (1997) *Nature Biotechnol.*, 15, 1271-1275). Monomeric fractions of E1, A2 and G4 scFv fragments bound to ED-B with affinity in the 107 - 108 M-1 range (Table 1).

As a further test of antibody specificity and usefulness, a 2D-PAGE immunoblot was performed, running on gel a lysate of the human melanoma cell line COLO-38, to which minute amounts of the ED-B containing recombinant 7B89 protein had been added (Figure 2). ScFv(E1) stained strongly and specifically only the 7B89 spot.

Antibodies E1, A2 and G4 were used to immunolocalise ED-B containing fibronectin (B-FN) in cryostat sections of glioblastoma multiforme, an aggressive human brain tumour with prominent angiogenetic processes. Figure 3 shows serial sections of glioblastoma multiforme, with the typical glomerulus-like vascular structures stained in red by the three antibodies. Immunostaining of sections of glioblastoma multiforme samples frozen in liquid nitrogen immediately after removal by surgical procedures, was performed as described (Carnemolla et al. (1996). *Int. J. Cancer*, 68, 397-405, Castellani et al. (1994). *Int. J. Cancer*, 59, 612-618). In short, immunostaining was performed using M2-anti-FLAG antibody (IBI Kodak), biotinylated anti-mouse polyclonal antibodies (Sigma), a streptavidin-biotin alkaline phosphatase complex staining kit (BioSpa, Milan, Italy) and naphtol-AS-MX-phosphate and fast-red TR (Sigma). Gill's hematoxylin was used as a counter-stain, followed by mounting in glycergel (Dako, Carpenteria, CA) as previously reported (Castellani et al. (1994). *Int. J. Cancer*, 59, 612-618).

Using similar techniques and the antibody L19 (see next example) we could also specifically stain new-forming blood vessels induced by implanting in the rabbit cornea polymer pellets soaked with angiogenic substances, such as vascular endothelial growth factor or phorbol esters.

5 Example 2

Isolation of a human scFv antibody fragment binding to the ED-B with sub-nanomolar affinity

ScFv(E1) was selected to test the possibility of improving its affinity with a limited number of mutations of CDR residues located at the periphery of the antigen 10 binding site (Figure 1A). We combinatorially mutated residues 31-33, 50, 52 and 54 of the antibody VH, and displayed the corresponding repertoire on filamentous phage. These residues are found to frequently contact the antigen in the known 15 3D-structures of antibody-antigen complexes. The resulting repertoire of  $4 \times 10^8$  clones was selected for binding to the ED-B domain of fibronectin. After two 20 rounds of panning, and screening of 96 individual clones, an antibody with 27-fold improved affinity was isolated (H10; Tables 1 and 2). Similarly to what others have 25 observed with affinity-matured antibodies, the improved affinity was due to slower dissociation from the antigen, rather than by improved kon values (Schier et al. (1996). Gene, 169, 147-155, Ito (1995). J. Mol. Biol., 248, 729-732). The antibody light chain is often thought to contribute less to the antigen binding affinity as supported by the fact that both natural and artificial antibodies devoid of light chain can still bind to the antigen (Ward et al. (1989) Nature, 341, 544-546, Hamers-Casterman et al. (1993). Nature, 363, 446-448). For this reason we chose to randomise only two residues (32 and 50) of the VL domain, which are centrally 30 located in the antigen binding site (Figure 1a) and often found in 3D structures to contact the antigen. The resulting library, containing 400 clones, was displayed on phage and selected for antigen binding. From analysis of the dissociation profiles using real-time interaction analysis with a BIACore instrument (Jonsson et al. (1991). BioTechniques, 11, 620-627) and koff measurements by competition experiments with electrochemiluminescent detection a clone (L19) was identified, that bound to the ED-B domain of fibronectin with a  $K_d = 54$  pM (Tables 1 and 2).

Affinity maturation experiments were performed as follows. The gene of scFv(E1) was PCR amplified with primers LMB1bis (5'-GCG GCC CAG CCG GCC ATG GCC GAG-3') and DP47CDR1for (5'-GA GCC TGG CGG ACC CAG CTC ATM NNM NNM NNGCTA AAG GTG AAT CCA GAG GCT G-3') to introduce random 5 mutations at positions 31-33 in the CDR1 of the VH (for numbering: 28), and with primers DP47CDR1back (5'-ATG AGC TGG GTC CGC CAG GCT CC-3') and DP47CDR2for (5'-GTC TGC GTA GTA TGT GGT ACC MNN ACT ACC MNN AAT MNN TGA GAC CCA CTC CAG CCC CTT-3') to randomly mutate positions 10 50,52,54 in CDR2 of the VH. The remaining fragment of the scFv gene, covering the 3'- portion of the VH gene, the peptide linker and the VL gene, was amplified 15 with primers DP47CDR2back (5'-ACA TAC TAC GCA GAC TCC GTG AAG-3') and JforNot (5'-TCA TTC TCG ACT TGC GGC CGC TTT GAT TTC CAC CTT GGT CCC TTG GCC GAA CG-3') (94°C 1 min, 60 C 1 min, 72 C 1 min). The three resulting PCR products were gel purified and assembled by PCR (21) with primers 20 LMB1bis and JforNot (94°C 1 min, 60 C 1 min, 72 C 1 min). The resulting single PCR product was purified from the PCR mix, double digested with NotI/Ncol and ligated into NotI/Ncol digested pDN332 vector. Approximately 9 µg of vector and 3 µg of insert were used in the ligation mix, which was purified by phenolisation and ethanol precipitation, resuspended in 50 µl of sterile water and electroporated in 25 electrocompetent TGI E.coli cells. The resulting affinity maturation library contained  $4 \times 10^8$  clones. Antibody-phage particles, produced as described (Nissim et al. (1994). EMBO J., 13, 692-698) were used for a first round of selection on 7B89 coated imunotube (Carnemolla et al. (1996). Int. J. Cancer, 68, 397-405). The selected phages were used for a second round of panning performed with 30 biotinylated ED-B, followed by capture with streptavidin coated magnetic beads (Dynal, Oslo, Norway; see previous paragraph). After selection, approximately 25% of the clones were positive in soluble ELISA (see previous chapter for experimental protocol). From the candidates positive in ELISA, we further identified the one (H10; Table 1) with lowest koff by BIACore analysis (Jonsson et al. (1991), BioTechniques, 11, 620-627).

The gene of scFv(H10) was PCR amplified with primers LMB1bis and DPKCDR1for (5'-G TTT CTG CTG GTA CCA GGC TAA MNN GCT GCT GCT

AAC ACT CTG ACT G) to introduce a random mutation at position 32 in CDR1 of the VL (for numbering: Chothia and Lesk (1987) *J.Mol.Biol.*, 196, 901-917), and with primers DPKCDR1back (5'-TTA GCC TGG TAC CAG CAG AAA CC-5') and DPKCDR2for (5'-GCC AGT GGC CCT GCT GGA TGC MNN ATA GAT GAG GAG 5 CCT GGG AGC C-3') to introduce a random mutation at position 50 in CDR2 of the VL. The remaining portion of the scFv gene was amplified with oligos DPKCDR2back (5'-GCA TCC AGC AGG GCC ACT GGC-3') and JforNot (94C 1 min, 60 C 1 min, 72 C 1 min) The three resulting products were assembled, digested and cloned into pDN332 as described above for the mutagenesis of the 10 heavy chain. The resulting library was incubated with biotinylated ED-B in 3% BSA for 30 min., followed by capture on a streptavidin-coated microtitre plate (Boehringer Mannheim GmbH, Germany) for 10 minutes. The phages were eluted with a 20 mM DTT solution (1,4-Dithio-DL-threitol, Fluka) and used to infect exponentially growing TG1 cells.

15 Analysis of ED-B binding of supernatants from 96 colonies by ELISA and by BIACore allowed the identification of clone L19. Anti-ED-B E1, G4, A2, H10 and L19 scFv antibody fragments selectively stain new-forming blood vessels in sections of aggressive tumours (Figure 3).

The above mentioned anti-ED-B antibody fragments were then produced 20 inoculating a single fresh colony in 1 liter of 2xTY medium as previously described in Pini et al. ((1997), *J. Immunol. Meth.*, 206, 171-182) and affinity purified onto a CNBr-activated sepharose column (Pharmacia, Uppsala, Sweden), which had been coupled with 10 mg of ED-B containing 7B89 recombinant protein (Carnemolla et al. (1996). *Int. J. Cancer*, 68, 397-405). After loading, the column 25 was washed with 50 ml of equilibration buffer (PBS, 1 mM EDTA, 0.5 M NaCl). Antibody fragments were then eluted with triethylamine 100 mM, immediately neutralised with 1M Hepes, pH 7, and dialysed against PBS. Affinity measurements by BIACore were performed with purified antibodies as described (Neri et al. (1997). *Nature Biotechnol.*, 15 1271-1275) [Figure 4]. Band-shift 30 analysis was performed as described (Neri et al. (1996). *Nature Biotechnology*, 14, 385-390), using recombinant ED-B fluorescently labelled at the N-terminal extremity (Carnemolla et al. (1996). *Int. J. Cancer*, 68, 397-405, Neri et al. (1997) .

Nature Biotechnol., 15 1271-1275) with the infrared fluorophore Cy5 (Amersham) [Figure 4]. BIAcore analysis does not always allow the accurate determination of kinetic parameters for slow dissociation reactions due to possible rebinding effects, baseline instability and long measurement times needed to ascertain that

5 the dissociation phase follows a single exponential profile. We therefore performed measurements of the kinetic dissociation constant  $k_{off}$  by competition experiments (Neri et al. (1996), Trends in Biotechnol., 14, 465-470) [Figure 4]. In brief, anti-ED-B antibodies (30 nM) were incubated with biotinylated ED-B (10 nM) for 10 minutes, in the presence of M2 anti-FLAG antibody (0.5 µg/ml) and polyclonal anti-

10 mouse IgG (Sigma) which had previously been labelled with a rutenium complex as described (Deaver, D. R. (1995). Nature, 377, 758-760). To this solution, in parallel reactions, unbiotinylated ED-B (1 µM) was added at different times. Streptavidin-coated dynabeads, diluted in Origen Assay Buffer (Deaver, D.R. (1995). Nature, 377, 758-760) were then added (20 µl, 1 mg/ml), and the resulting

15 mixtures analysed with a ORIGEN Analyzer (IGEN Inc. Gaithersburg, MD USA). This instrument detects an electrochemiluminescent signal (ECL) which correlates with the amount of scFv fragment still bound to the biotinylated ED-B at the end of the competition reaction. Plot of the ECL signal versus competition time yields a profile, that can be fitted with a single exponential with characteristic constant  $k_{off}$

20 [Figure 4; Table 2].

### Example 3

#### Targeting tumours with a high-affinity radiolabelled scFv specific for the ED-B domain of fibronectin

Radioiodinated scFv(L19) or scFv(D1.3) (an irrelevant antibody specific for hen egg lysozyme) were injected intravenously in mice with subcutaneously implanted murine F9 teratocarcinoma, a rapidly growing aggressive tumour. Antibody biodistributions were obtained at different time points (Figure 4). ScFv(L19) and scFv(D1.3) were affinity purified on an antigen column (Neri et al. (1997, Nature Biotechnol. 15, 1271-1273) and radiolabelled with iodine-125 using the Iodogen method (Pierce, Rockford, IL, USA). Radiolabelled antibody fragments retained > 80% immunoreactivity, as evaluated by loading the radiolabelled antibody onto an antigen column, followed by radioactive counting of the flow-through and eluate

fractions. Nude mice (12 weeks old Swiss nudes, males) with subcutaneously-implanted F9 murine teratocarcinoma (Neri et al. (1997) *Nature Biotechnol.* 15, 1271-1273) were injected with 3 µg (3-4 µCi) of scFv in 100 µl saline solution. Tumour size was 50-250 mg, since larger tumours tend to have a necrotic centre.

5 However, targeting experiments performed with larger tumours (300-600 mg) gave essentially the same results. Three animals were used for each time point. Mice were killed with humane methods, and organs weighed and radioactively counted. Targeting results of representative organs are expressed as percent of the injected dose of antibody per gram of tissue (% ID / g). ScFv(L19) is rapidly eliminated  
10 from blood through the kidneys; unlike conventional antibodies, it does not accumulate in the liver or other organs. Eight percent of the injected dose per gram of tissue localises on the tumour already three hours after injection; the subsequent decrease of this value is due to the fact that the tumour doubles in size in 24-48 hours. Tumour:blood ratios at 3, 5 and 24 hours after injection were  
15 1.9, 3.9 and 11.8 respectively for L19, but always below 1.0 for the negative control antibody.

Radiolabelled scFv(L19) preferentially localises on tumours already few hours after injection, suggesting its usefulness for the immunoscintigraphic detection of angiogenesis in patients.

20 **Example 4**

**Anti-ED-B antibodies selectively stain newly-formed ocular blood vessels**

Angiogenesis, the formation of new blood vessels from pre-existing ones, is a characteristic process which underlies many diseases, including cancer and the majority of ocular disorders which result in loss of vision. The ability to selectively target and occlude neovasculature will open diagnostic and therapeutic opportunities.

We investigated whether B-FN is a specific marker of ocular angiogenesis and whether antibodies recognising B-FN could selectively target ocular neovascular structures in vivo upon systemic administration. To this aim we stimulated  
30 angiogenesis in the rabbit cornea, which allows the direct observation of new-blood vessels, by surgically implanting pellets containing vascular endothelial growth factor or a phorbol ester (Figure 7). Sucralfate (kind gift of Merck,

Darmstadt, Germany) / hydron pellets containing either 800 ng vascular endothelial growth factor (Sigma) or 400 ng phorbol 12-myristate 13-acetate («PMA»; Sigma) were implanted in the cornea of New Zealand White female rabbits as described [D'Amato, R.J., et al., *Proc. Natl. Acad. Sci. USA* 91, 4082-5 4085 (1994)]. Angiogenesis was induced by both factors. Rabbits were monitored daily. With both inducers newly formed blood vessels were strongly ED-B-positive in immunohistochemistry. For all further experiments, PMA pellets were used. Immunohistochemical studies showed that L19 strongly stains the neovasculature induced in the rabbit cornea (Fig. 8; 9a), but not pre-existing blood vessels of the 10 eye (Fig. 9b, c) and of other tissues (data not shown). Immunohistochemistry was performed as described [Carnemolla, B. et al., *Int. J. Cancer* 68, 397-405 (1996)].

#### Example 5

The human antibody fragment L19, binding to the ED-B with sub-nanomolar affinity, targets ocular angiogenesis *in vivo*

15 Using the rabbit cornea model of angiogenesis described in the previous example, and an immunophotodetection methodology [Neri, D. et al., *Nature Biotechnol.* 15, 1271-1275 (1997)], we demonstrated that L19, chemically coupled to the red fluorophore Cy5, but not the antibody fragment (HyHEL-10)-Cy5 directed against an irrelevant antigen (Fig. 10a,b), selectively targets ocular angiogenesis upon 20 intravenous injection. Fluorescent staining of growing ocular vessels was clearly detectable with L19 immediately after injection, and persisted for at least two days analogous to previous observations with tumour angiogenesis. Subsequent ex vivo immunofluorescent microscopic analysis on cornea sections confirmed the localisation of L19, but not of HyHEL-10, around vascular structures (Fig. 10c,d).  
25 The demonstration of the antibody-based selective targeting of ocular neovascularisation, together with the reactivity of anti-B-FN antibodies in different species, warrants future clinical investigations. Immunofluorescence imaging could be useful for the early detection of ocular angiogenesis in risk patients, before lesions become manifest in fluoroangiography.  
30 Some methodological details:  
For ex vivo immunofluorescence and for some H/E stainings, corneas were fixed in 4% paraformaldehyde in PBS before embedding. Fluorescence photodetection

experiments were performed with rabbits sedated using 5 mg/kg Acepromazin. For targeting experiments, 3.5 mg of scFv(L19)<sub>1</sub>-Cy5<sub>0.66</sub> and 2.8 mg of scFv(HyHEL-10)<sub>1</sub>-Cy5<sub>0.83</sub> were injected intravenously in each rabbit (injection time = 15 min). A strong fluorescence in the corneal neovasculature was observed already 5 immediately after injection of L19, but not of HyHEL-10, and persisted for several hours. As an additional test of specificity, rabbits injected the previous day with scFv(HyHEL-10)-Cy5 and negative in the fluorescence photodetection, were injected the next day with scFv(L19)-Cy5, and showed a strong fluorescent staining of corneal angiogenesis.

10 For fluorescence detection, the eye was illuminated with a tungsten halogen lamp (model Schott KL1500; Zeiss, Jena, Germany) equipped with a Cy5-excitation filter (Chroma, Brattleboro, VT, U.S.A.) and with two light guides whose extremities were placed at approximately 2 cm distance from the eye. Fluorescence was detected with a cooled C-5985 monochrome CCD-camera (Hamamatsu, 15 Hamamatsu-City, Japan), equipped with C-mount Canon Zoom Lens (V6x16; 16-100 mm; 1: 1.9) and a 50 mm diameter Cy5 emission filter (Chroma), placed at 3-4 cm distance from the irradiated eye. Acquisition times were 0.4 s.

Cy5 fluoroangiography experiments were performed with the same experimental set up, but injecting intravenously 0.25 mg Cy5-Tris (the reaction product between 20 Cy5-NHS and tris[hydroxymethyl]aminomethane; injection time = 5 s). Acquisition times were 0.2 s.

Antibody fragments were in scFv format. The purification of scFv(L19) and scFv(HyHEL-10) and their labeling with the N-hydroxysuccinimide (NHS) esters of indocyanine dyes have been described elsewhere [Neri, D. et al., *Nature Biotechnol.* 15, 1271-1275 (1997); Fattorusso, R., et al. (1999) *Structure*, 7, 381-25 390]. Antibody : Cy5 labeling ratios for the two antibodies were 1.5 : 1 and 1.2 : 1, respectively. Cy5-NHS was purchased from Amersham Pharmacia Biotech (Zurich, Switzerland), ovalbumin from Sigma (Buchs, Switzerland).

After the labeling reaction, antibody conjugates were separated from 30 unincorporated fluorophore or photosensitiser using PD-10 columns (Amersham Pharmacia Biotech) equilibrated in 50 mM phosphate, pH 7.4, 100 mM NaCl (PBS). Immunoreactivity of antibody conjugates was measured by affinity

chromatography on antigen columns [Neri, D. et al., *Nature Biotechnol.* 15, 1271-1275 (1997)] and was in all cases > 78%. Immunoconjugates were analysed by sodium dodecyl sulfate polyacrylamide gel electrophoresis and migrated as a band of MW = 30'000 Dalton (purity = 90%).

5 Example 6

The human antibody fragment L19, chemically conjugated to the photosensitiser Sn (IV) chlorine e6, selectively targets ocular angiogenesis and mediates its occlusion upon irradiation with red light

To test whether selective vessel ablation could be achieved by virtue of the 10 antibody-mediated targeting, we injected rabbits with the L19 antibody fragment or an irrelevant protein that does not localise in newly formed blood vessels (ovalbumin) coupled to the photosensitiser tin (IV) chlorin e<sub>6</sub> (hereafter named «PS»). The eyes of injected animals were irradiated with red light (light dose = 78 J/cm<sup>2</sup>). Representative results are depicted in Figure 11. A striking macroscopic 15 difference was observed 16 h after irradiation in rabbits treated with L19-PS (Fig. 11a,b), with coagulation of the corneal neovasculature but not of vessels in the conjunctiva or in other ocular structures. Fluoroangiography with the indocyanine fluorophore Cy5 (Fig. 11c) confirmed vessel occlusion as a characteristic hypofluorescent area. On the contrary, hyperfluorescent areas were observed in 20 the leaky neovasculature of non-irradiated eyes (Fig. 11d,h). No macroscopic alteration was detectable in the irradiated vessels of rabbits treated with ovalbumin-PS (Fig. 11e-g), either ophthalmoscopically or by Cy5 fluoroangiography. The effect of irradiation of the targeted L19-PS conjugate at 25 early stages of corneal angiogenesis are shown in Fig. 11i-l. Selectively coagulated blood vessels were macroscopically visible in live animals (Fig. 11i,j) and even more evident in animals immediately after euthanasia (Fig. 11k,l).

Photodynamic damage was further investigated using microscopic techniques. After irradiation, vessel occlusion could be detected by standard hematoxylin/eosin (H/E) staining techniques in both non-fixed and paraformaldehyde-fixed cornea 30 sections of animals treated with L19-PS (Fig. 11b,f,j), but not of those treated with ovalbumin-PS (Fig. 11a,e,i). Apoptosis in the portion of the cornea targeted by the photosensitiser conjugate was clearly visible in the fluorescent TUNEL assay (Fig.

11c,g), but hardly detectable in negative controls (Fig. 11d,h). A higher magnification view showed apoptosis of endothelial cells in vascular structures (Fig. 11g). No damage to blood vessels of the iris, sclera and conjunctiva of treated animals could be observed either by TUNEL assay (not shown) or by H/E staining (Fig. 11k,l).

Selective photodynamic ablation of neovasculature promises to be beneficial for the treatment of ocular disorders and of other angiogenesis-related pathologies that are accessible to irradiation using light diffusers or fibre optic techniques. The results of this study clearly demonstrate that ocular neovasculature can be selectively occluded without damaging pre-existing blood vessels and normal tissues.

Some methodological details:

Tin (IV) chlorin e<sub>6</sub> was selected from a panel of photosensitisers, on the basis of their potency, solubility and specificity, after coupling to a rabbit anti-mouse polyclonal antibody (Sigma). These immunoconjugates were screened by targeted photolysis of red blood cells coated with a monoclonal antibody specific for human CD47 (#313441A; Pharmingen, San Diego CA, U.S.A.). Tin (IV) chlorin e<sub>6</sub> was prepared as described [Lu, X.M. et al., *J. Immunol. Methods* 156, 85-99 (1992)]. For coupling to proteins, tin (IV) chlorin e<sub>6</sub> (2 mg/ml) was mixed for 30 min at room temperature in dimethylformamide with a ten-fold molar excess of EDC (N'-3-dimethylaminopropyl-N-ethylcarbodiimide hydrochloride, Sigma) and NHS (N-hydroxysuccinimide, Sigma). The resulting activated mixture was then added to an eight-fold larger volume of protein solution (1 mg/ml) and incubated at room temperature for 1h.

After the labeling reaction, antibody conjugates were separated from unincorporated fluorophore or photosensitiser using PD-10 columns (Amersham Pharmacia Biotech) equilibrated in 50 mM phosphate, pH 7.4, 100 mM NaCl (PBS). Immunoreactivity of antibody conjugates was measured as described in the previous Example.

For photokilling experiments, rabbits were injected intravenously with 12 mg scFv(L19)<sub>1</sub> -tin (IV) chlorin e<sub>6</sub><sub>0.8</sub> or 38 mg ovalbumin<sub>1</sub> – tin (IV) chlorin e<sub>6</sub><sub>0.36</sub>, and kept in the dark for the duration of the experiment. Eight hours after injection,

rabbits were anaesthetised with ketamin (35 mg/kg) / xylazine (5 mg/kg) / acepromazin (1 mg/kg), and one of the two eyes was irradiated for 13 min with a Schott KL1500 tungsten halogen lamp equipped with a Cy5 filter (Chroma) and with two light guides whose extremities were placed at 1 cm distance from the eye.

5 The illuminated area was approximately 1 cm<sup>2</sup>, with an irradiation power density of 100 mW/cm<sup>2</sup>, measured using a SL818 photodetector (Newport Corp., Irvine, CA, U.S.A.). No sign of animal discomfort after irradiation was observed. As a preventive measure, rabbits received analgesics after irradiation (buprenorphine 0.03 mg/Kg). To monitor photokilling, eyes were investigated with an

10 ophthalmoscope and photographed using a fundus camera KOWA SL-14 (GMP SA, Rennens, Lausanne, Switzerland). Five rabbits were treated with each of the tin (IV) chlorin e<sub>6</sub> conjugates and irradiated in one eye only, the other eye serving as an internal negative control. As additional control, two rabbits were irradiated only, but received no photosensitiser conjugate.

15 Immediately after rabbits' euthanasia with an overdose of anaesthetic, eyes were enucleated, corneas removed, then embedded in Tissue Tek (Sakura Finetechnical, Tokyo, Japan) and frozen. For ex vivo immunofluorescence and for some H/E stainings, corneas were fixed in 4% paraformaldehyde in PBS before embedding. Cryostat sections of 5 µm were used for further microscopic analysis.

20 Fluorescent TUNEL assays were performed according to manufacturer's instructions (Roche Diagnostic, Rotkreuz, Switzerland).

Example 7

Conjugation of astatine-211 to human antibody fragment L19 through m-MeATE

A solution of m-bromobenzoic acid (1 g, 5 mmol) in 25 ml of dry tetrahydrofuran (THF) is placed in a 250 ml, two-necked round bottom flask, maintained under nitrogen atmosphere and cooled to ~ 75 °C using (ether:dry ice) bath. To the above, 6.25 ml of n-buthyl lithium (1.6M solution in hexane) is added slowly over 25 min. The dilithio anion thus generated is stirred for an additional 10 min. Still under a nitrogen atmosphere, trimethylstannyl chloride (1.09 mg, 5.47 mmol) dissolved in 10 ml dry THF is added over 20 min to the reaction mixture. The cooling bath is removed and the reaction is slowly brought to room temperature (RT) and stirring is kept for 1 hour. The reaction is quenched by addition of water

(10 ml) and extracted three times with 100 ml of diethyl ether. The organic phase is washed with 5% NaHCO<sub>3</sub> (2 x 25 ml) and water (2 x 20 ml). After drying over MgSO<sub>4</sub>, it is concentrated on a rotary evaporator. Thin layer chromatography (TLC) is performed on analytical, pre-coated silica gel plastic plates using the following mobile phase: Hexane:ethylacetate(EtOAc):acetic acid (AcOH) (70:29.7:0.3). 3-(trimethylstannyl) benzoate (R<sub>f</sub> = 0.46) is purified by gravimetric chromatography using a silica gel 60 column (40-63  $\mu$ , 200 x 3 mm) eluted with the same phase above reported. We obtain 100 mg (0.35 mmol) of product, in 7% yield as an oil. The assigned structure (<sup>1</sup>H-NMR) is reported in Figure 17a,b.

10 To the stannyl ester resuspended in THF (10 ml), N-hydroxy-succinimide (48.34 mg, 0.42 mmol) and diclohexylcarbodiimide (86.66 mg, 0.42 mmol) are added and stirred overnight at room temperature. Precipitated dicyclohexylurea is filtered off and the solvent is evaporated on a rotary evaporator to give an oil. The desired m-MeATE (R<sub>f</sub> = 0.34) is isolated by gravimetric chromatography with

15 Hexane:EtOAc (2:1) using a silica gel 60 column. After evaporation of the solvent we obtain 92.3 mg (0.241 mmol) of m-MeATE in 68.8% relative yield. The assigned structure is confirmed by <sup>1</sup>H-NMR and Mass Spectroscopy (Figures 18a,b and 19). This bifunctional compound is used to couple scFv(L19) to the alpha-emitting radionuclide Astatine-211.

20 In a glove-box previously inflated with inert gas, 1.9 mg of m-MeATE (5 $\mu$ mol) and *tert*-butyl hydroperoxide (20  $\mu$ mol) are added to the chloroform trap containing 1 mCi <sup>211</sup>At anion. The reaction is kept at room temperature for 15 minutes and the mixture is purified using a disposable Sep-Pak silica gel cartridge. The reaction mixture is added to 300  $\mu$ l of Hexane and loaded on the column previously

25 equilibrated with Hexane. Following washing with Hexane (40 ml) and 8% ethylacetate in Hexane (25 ml), the product N-succinimidyl 3-<sup>211</sup>At-benzoate is isolated in 30% ethylacetate in Hexane (ca. 15 ml). The radionuclide incorporation in the bifunctional agent m-MeATE is measured using an automated gamma counter with an energy window set to include the Polonium K X-rays emitted in the

30 decay of <sup>211</sup>At. The eluted fraction is evaporated and resuspended in dimethyl sulfoxide (100  $\mu$ l) and then added to 200  $\mu$ l of borate buffer (pH = 8.5) containing 13 nmoles of scFv (L19). The reaction is stirred at room temperature for 30

minutes and the L19-<sup>211</sup>At conjugate is purified using a PD-10 disposable gel filtration column. Antibody immunoreactivity after labeling is evaluated by loading an aliquot of radiolabeled sample onto 200  $\mu$ l of ED-B-Sepharose resin (capacity, > 2.5 mg ED-B/ml resin) on a pasteur pipette, followed by radioactive counting of 5 the flow-through and eluate fractions. Immunoreactivity, defined as the ratio between the counts of the eluted protein and the sum of the counts of the eluted and flow-through fractions, is > 80%.

**Table 1:**

Sequences of selected anti-ED-B antibody clones

		VH chain			VL chain		
5	Clone	31-33*	50-54*	95-98*	32*	50*	91-96*
	A2	SYA	AISGSG	GLSI	Y	G	NGWYPW
	G4	SYA	AISGSG	SFSF	Y	G	GGWL PY
10	E1	SYA	AISGSG	FPPF Y	Y	G	TGRIIPP
	H10	SFS	SIRGSS	FPPF Y	Y	G	TGRIIPP
	L19	SFS	SIRGSS	FPPF Y	Y	Y	TGRIIPP

15

Relevant amino acid positions (\*: numbering according to Tomlinson et al. (1995) EMBO J., 14, 4628-4638) of antibody clones isolated from the designed synthetic libraries. Single amino acid codes are used according to standard IUPAC nomenclature.

20

**Table 2:**

Affinities of anti-ED-B scFv fragments

Clone	kon (s <sup>-1</sup> M <sup>-1</sup> )	koff (s <sup>-1</sup> ) <sup>B</sup>	koff (s <sup>-1</sup> ) <sup>C</sup>	K <sub>d</sub> (M)*
A2	1.5 x 10 <sup>5</sup>	2.8 x 10 <sup>-3</sup>	-	1.9 x 10 <sup>-8</sup>
G4	4.0 x 10 <sup>4</sup>	3.5 x 10 <sup>-3</sup>	-	8.7 x 10 <sup>-8</sup>
E1	1.6 x 10 <sup>5</sup>	6.5 x 10 <sup>-3</sup>	-	4.1 x 10 <sup>-8</sup>
H10	6.7 x 10 <sup>4</sup>	5.6 x 10 <sup>-4</sup>	9.9 x 10 <sup>-5</sup>	1.5 x 10 <sup>-9</sup>
L19	1.1 x 10 <sup>5</sup>	9.6 x 10 <sup>-5</sup>	6.0 x 10 <sup>-6</sup>	5.4 x 10 <sup>-11</sup>

5 \*) K<sub>d</sub> = k<sub>off</sub> / k<sub>on</sub>. For the high-affinity binders H10 and L19, k<sub>off</sub> values from BIAcore experiments are not sufficiently reliable due to effects of the negatively-charged carboxylated solid dextran matrix; K<sub>d</sub> values are therefore calculated from k<sub>off</sub> measurements obtained by competition experiments (Experimental Procedures).

10 20 k<sub>off</sub>, kinetic dissociation constant; k<sub>on</sub>, kinetic association constant; K<sub>d</sub>, dissociation constant. B = measured on the BIAcore; C = measured by competition with electrochemiluminescent detection. Values are accurate to +/- 50%, on the basis of the precision of concentration determinations.

## CLAIMS

1. An antibody with specific affinity for a characteristic epitope of the ED-B domain of fibronectin, wherein the antibody has improved affinity to said ED-B epitope.
2. The antibody according to claim 1, wherein the affinity is in the subnanomolar range.
3. The antibody according to claim 1, wherein the antibody recognizes ED-B(+) fibronectin.
4. The antibody according to claim 1, wherein said antibody is in the scFv format.
5. The antibody according to claim 4, the antibody being a recombinant antibody.
- 10 6. The antibody according to claim 4, wherein the affinity is improved by introduction of a limited number of mutations in its CDR residues.
7. The antibody according to claim 6, wherein the residues are residues 31-33, 50, 52 and 54 of VH and two residues 32 and 50 of its VL domain which have been mutated.
- 15 8. The antibody according to claim 1, wherein the antibody binds the ED-B domain of fibronectin with a Kd of 27 to 54 pM, most preferably with a Kd of 54 pM.
9. The antibody according to claim 1, being the antibody L19.
10. The antibody according to claim 1 with the following amino acid sequence:

VH

20 EVQLLESGGG LVQPGGSLRL SCAASGFTFS  
SFSMSWVRQA PGKGLEWVSS ISGSSGTTYY  
ADSVVKGRFTI SRDNSKNTLY LQMNSLRAED  
TAVYYCAKPF PYFDYWGQGT LVTVSS  
linker

25 GDGSSGGGGASTG

VL

EIVLTQSPGT LSLSPGERAT LSCRASQSVS  
SSYLAWYQQK PGQAPRLLIY YASSRATGIP  
DRFSGSGSGT DFTLTISRLE PEDFAVYYCQ

30 QTGRIPPTFG QGTKVEIK

- 11. The antibody according to claim 1, wherein the antibody is a functionally equivalent variant form of L19.
- 12. The antibody according to claim 9, wherein the antibody is radiolabelled.
- 13. The antibody according to claim 12, wherein the antibody is radioiodinated.

14. Method for rapid angiogenesis targeting wherein an antibody with specific affinity for a characteristic epitope of the ED-B domain of fibronectin, the antibody having improved affinity to said ED-B domain, is used.
15. Method according to claim 14 for immunoscintigraphic detection of angiogenesis.
16. Method according to claim 15 for detecting diseases characterized by vascular proliferation such as diabetic retinopathy, age-related macular degeneration or tumours.
17. Method according to claim 14, wherein the antibody localizes the respective tissue three to four hours, most preferably 3 hours after its injection.
18. A diagnostic kit comprising an antibody with specific affinity for a characteristic epitope of the ED-B domain of fibronectin, said antibody having improved affinity to said ED-B domain and one or more reagents necessary for detecting angiogenesis.
19. Method for diagnosis and therapy of tumours and diseases characterized by vascular proliferation wherein an antibody with specific affinity for a characteristic epitope of the ED-B domain of fibronectin, said antibody having improved affinity to said ED-B domain, is used.
20. Conjugates comprising an antibody according to Claim 1 and a molecule capable of inducing blood coagulation and blood vessel occlusion.
21. Conjugates according to claim 20 wherein the molecule capable of inducing blood coagulation and blood vessel occlusion is a photoactive molecule.
22. Conjugates according to claim 21 wherein the photoactive molecule is a photosensitizer.
23. Conjugates according to claim 22 wherein the photosensitizer absorbs at wavelength above 600 nm.
24. Conjugates according to claim 22 wherein the photosensitizer is a derivative of tin (IV) chlorine e6.
25. Conjugates according to claim 20 wherein the molecule capable of inducing blood coagulation and blood vessel occlusion is a radionuclide.
26. Conjugates according to claim 25 wherein the radionuclide is an  $\alpha$ - or  $\beta$ -emitting radionuclide.

27. Conjugates according to Claim 26 the  $\alpha$ -emitting radionuclide is astatine-211, bismuth-212, bismuth-213.
28. Conjugates according to claim 20 wherein the molecule capable of inducing blood coagulation and blood vessel occlusion is represented by a photosensitizer and a radionuclide.
29. Method for the treatment of angiogenesis-related pathologies wherein a conjugate according to claim 20 is injected.
30. Method for the treatment of angiogenesis-related pathologies wherein a conjugate according to claim 22 is injected, followed by irradiation.
31. Method according to claim 30 wherein the angiogenesis-related pathology treated is caused by or associated with ocular angiogenesis.
32. Method for the treatment of angiogenesis-related pathologies wherein a conjugate according to claim 25 is injected.
33. Method according to claim 32 wherein the radionuclide is astatine-211.
34. Method for the treatment of angiogenesis-related pathologies wherein a conjugate according to claim 28 is injected.
35. 3-(trimethylstannyl)benzoic acid

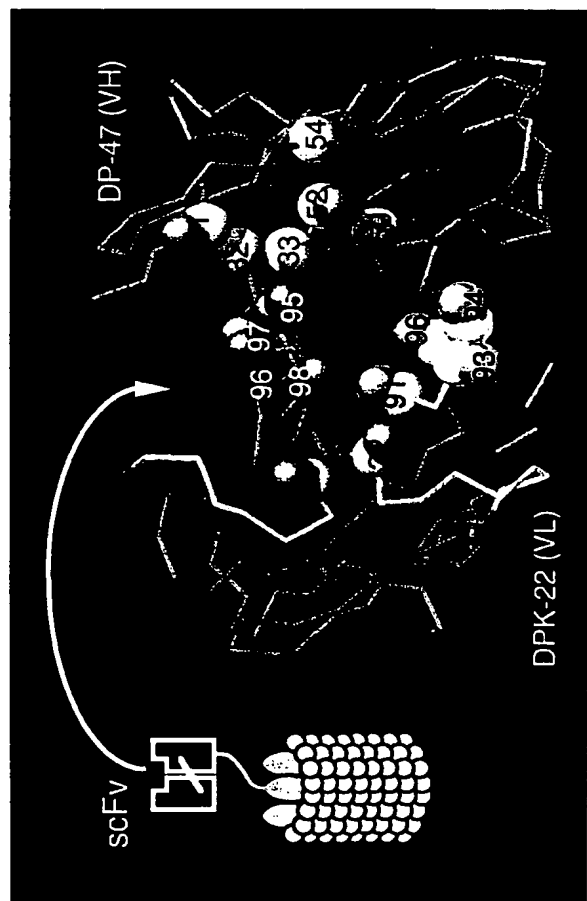
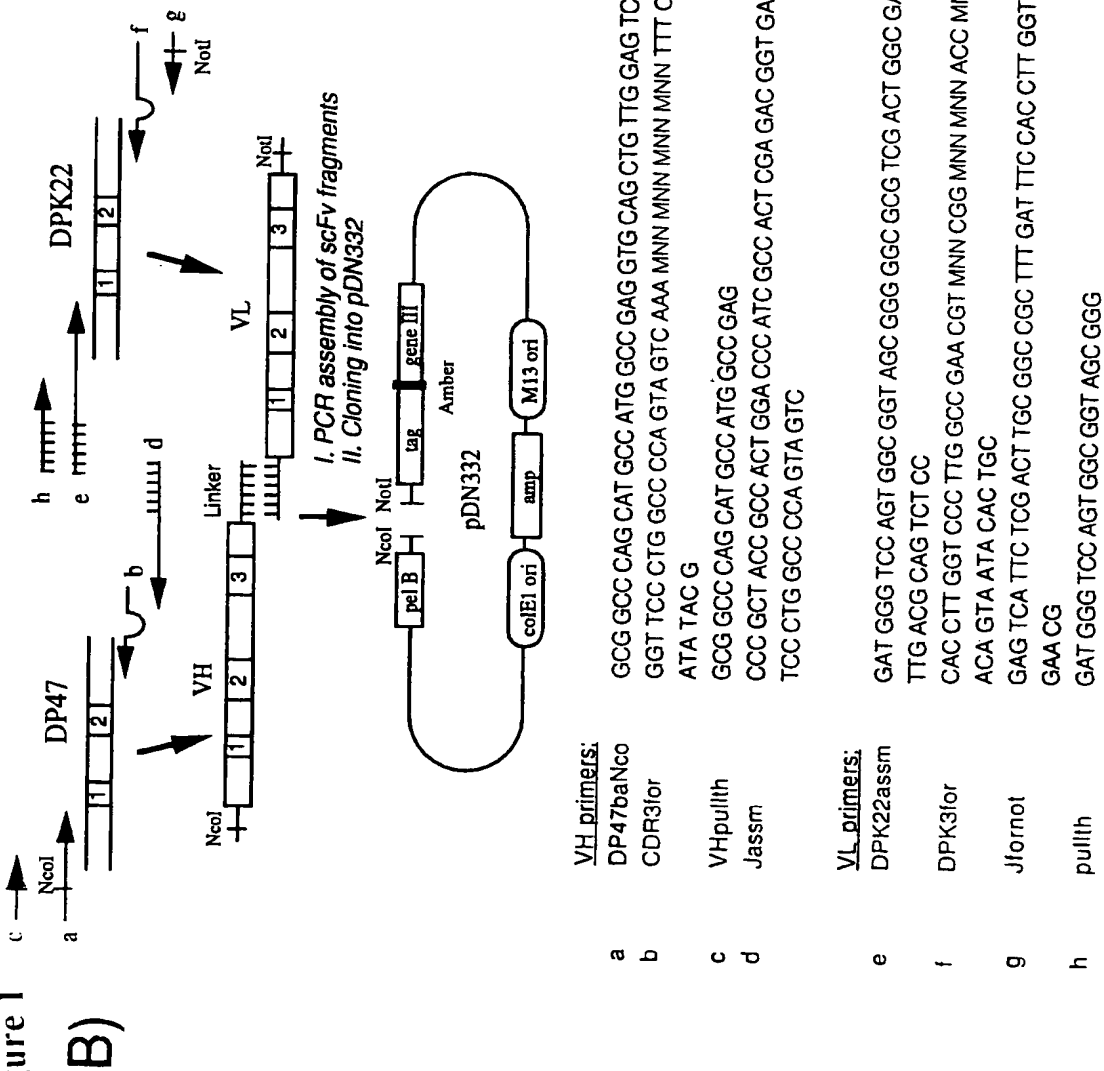


Figure 1  
A)

Figure 1



3/23

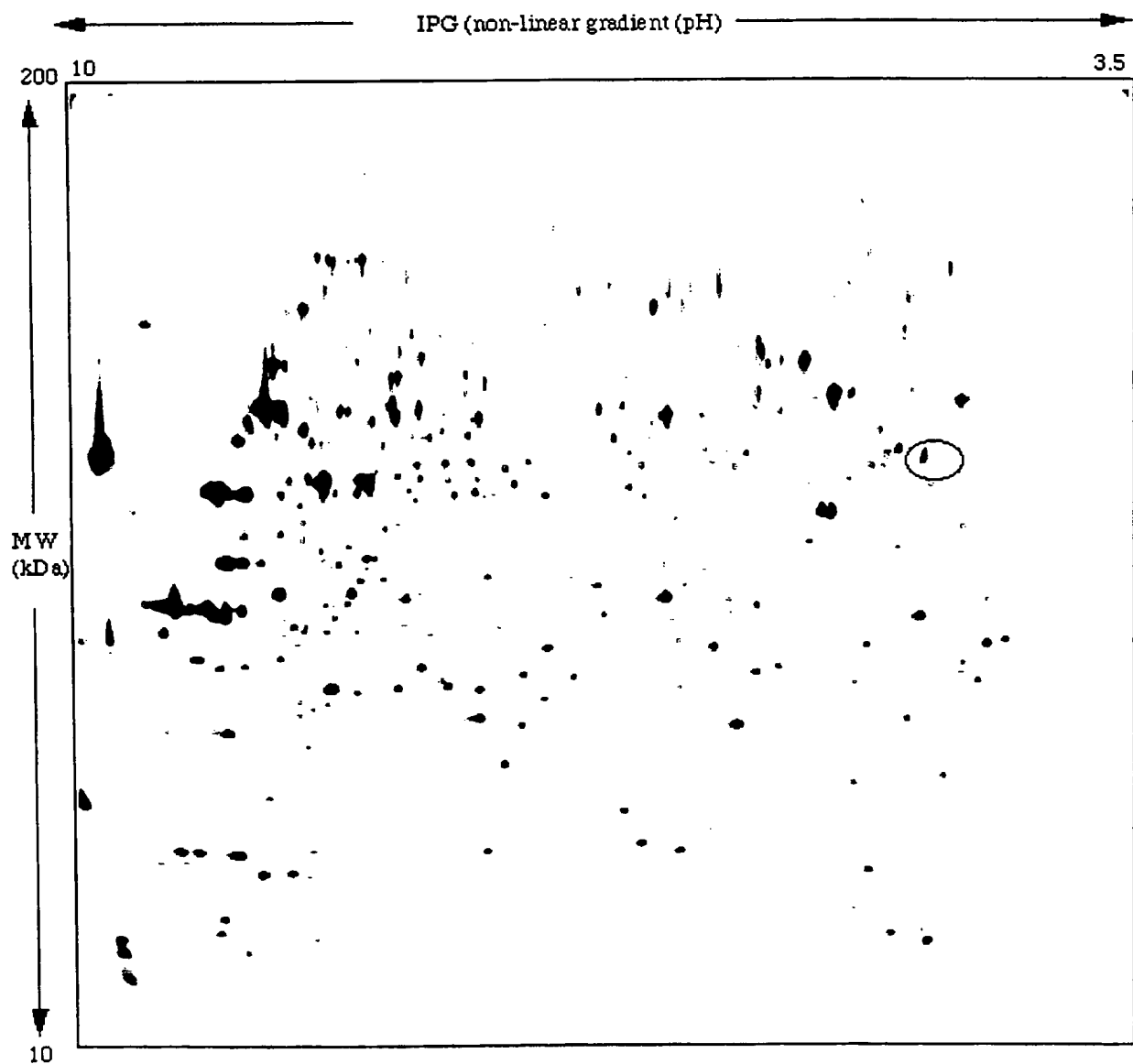


Figure 2a

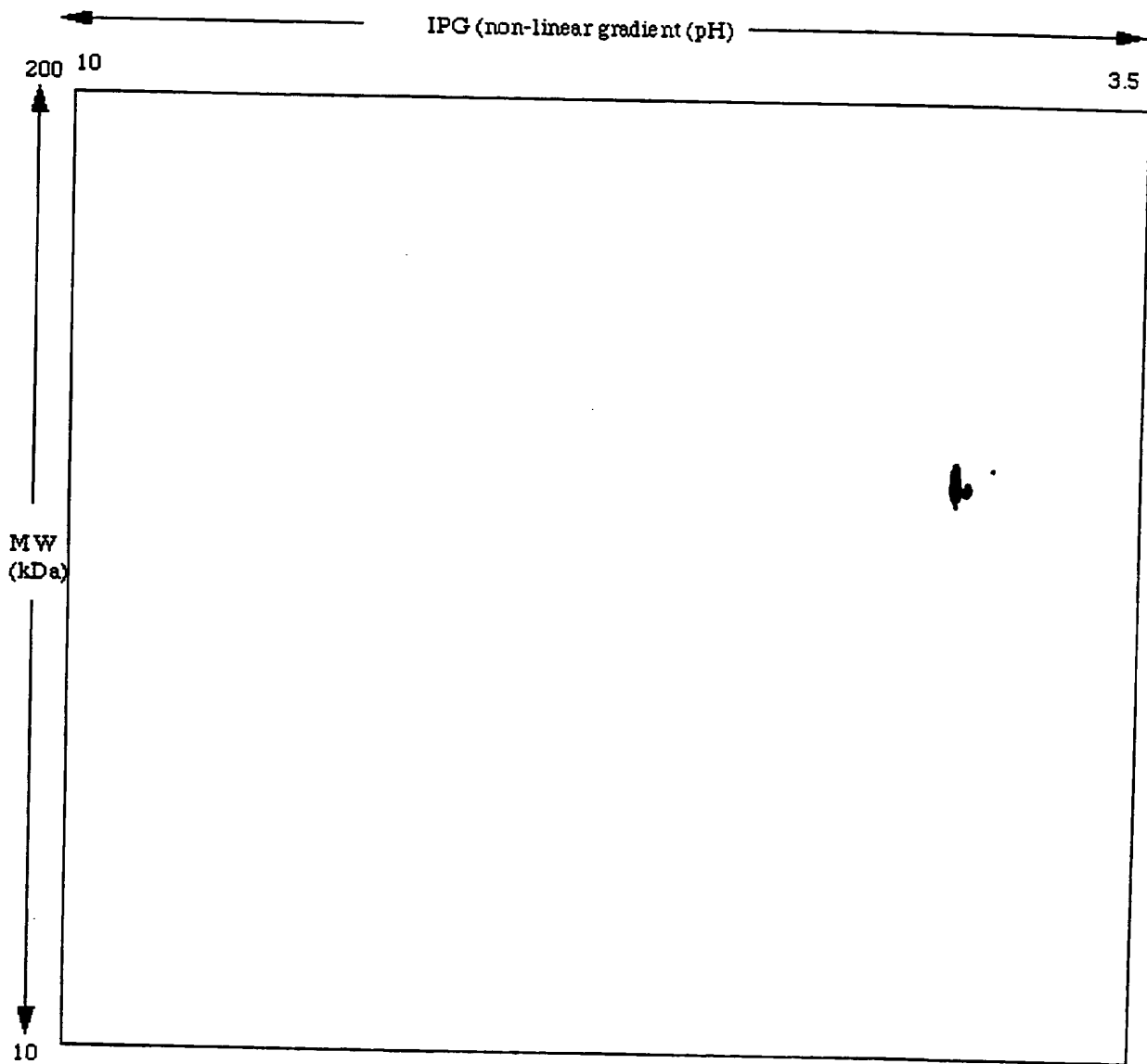
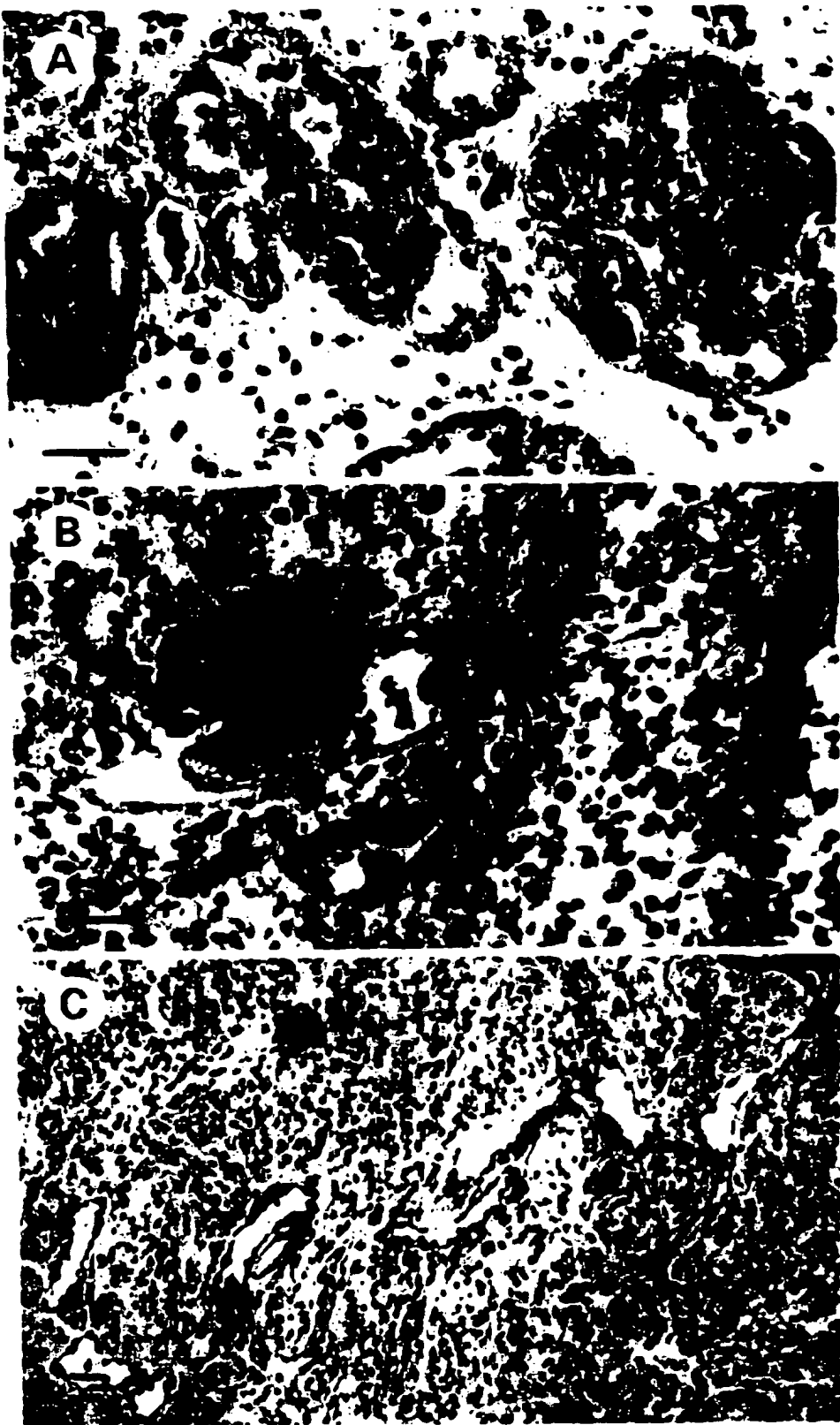


Figure 2b

Figure 3

5/23



6/23

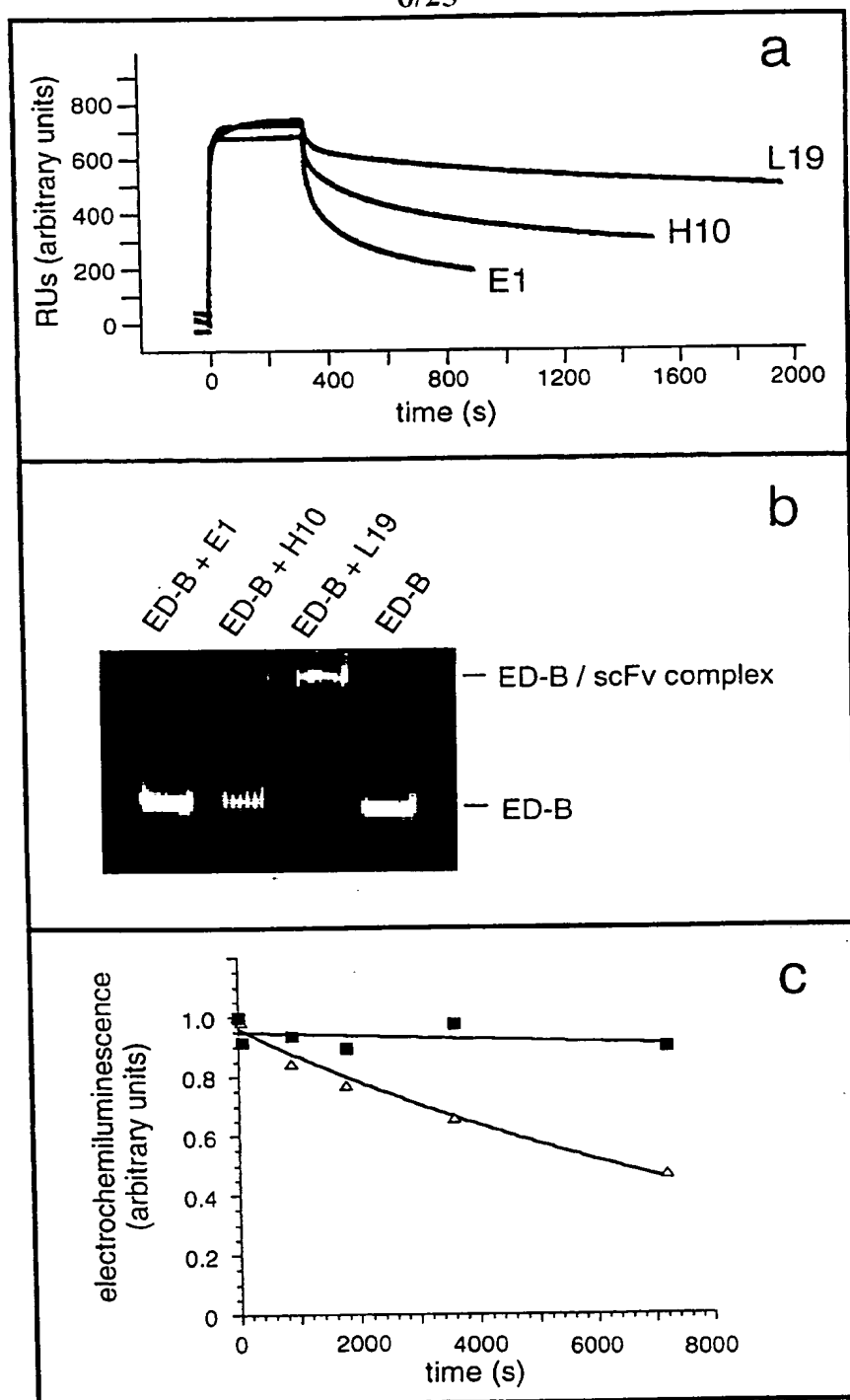
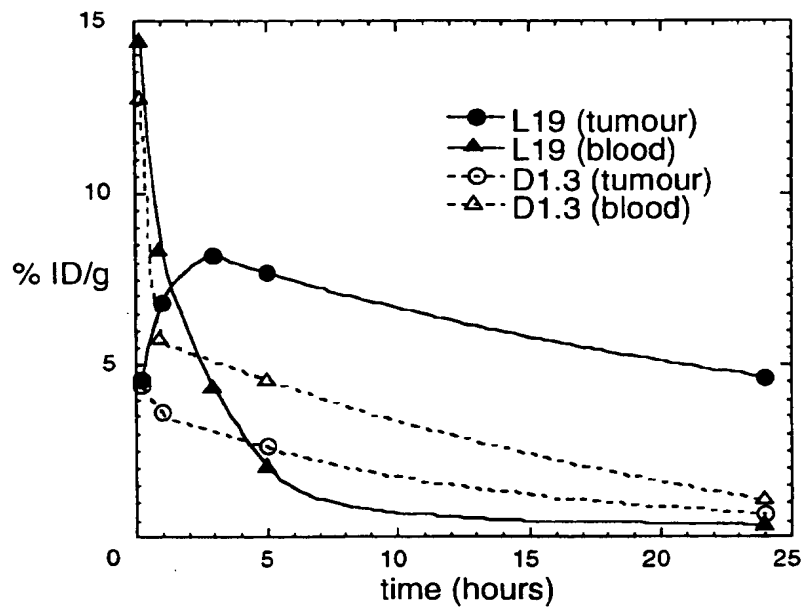


Figure 4



time (h)	scFv (L19)							scFv (D1.3)	
	Kidney	Spleen	Lung	Liver	Brain	Blood	Tumor	Blood	Tumor
0.25	26.4 ± 4.7	5.4 ± 0.4	15.1 ± 5.1	5.7 ± 0.6	0.4 ± 0.04	14.4 ± 2.6	4.6 ± 1.1	12.7 ± 0.1	4.4 ± 1.4
1	19.2 ± 3.9	3.8 ± 0.3	9.8 ± 0.9	2.8 ± 0.3	0.3 ± 0.1	8.3 ± 0.9	6.9 ± 2.4	5.7 ± 0.7	3.6 ± 1.0
3	8.1 ± 1.6	2.0 ± 0.3	5.0 ± 1.4	1.7 ± 0.02	0.2 ± 0.01	4.3 ± 0.3	8.2 ± 4.2	—	—
5	4.2 ± 1.1	1.8 ± 0.2	3.5 ± 0.2	1.3 ± 0.3	0.1 ± 0.02	2.1 ± 1.6	7.7 ± 2.5	4.6 ± 1.2	2.6 ± 1.5
24	0.7 ± 0.1	0.4 ± 0.1	1.0 ± 0.3	0.2 ± 0.04	0.02 ± 0.01	0.4 ± 0.1	4.7 ± 0.6	1.1 ± 0.5	0.7 ± 0.4

Figure 5

VH	E V Q L L E S G G G	L V Q P P G G S L R L	S C A A S G F T F S
	S F S M S W V R Q A	P G K G L E W V S S	I S G S S G T T Y Y
	A D S V K G R F T I	S R D N S K N T L Y	L Q M N S L R A E D
	T A V Y Y C A K P F	P Y F D Y W G Q G T	L V T V S S
linker	G D G S S G G S G G A S T G		
VL	E I V L T Q S P G T	L S L S P G E R A T	L S C R A S Q S V S
	S S Y L A W Y Q Q K	P G Q A P R L L I Y	Y A S S R A T G I P
	D R F S G S G S G T	D F T L T I S R L E	P E D F A V Y Y C Q
	Q T G R I P P T F G	Q G T K V E I K	

Amino acid sequence of antibody L19

Figure 6

Figure 7

9/23



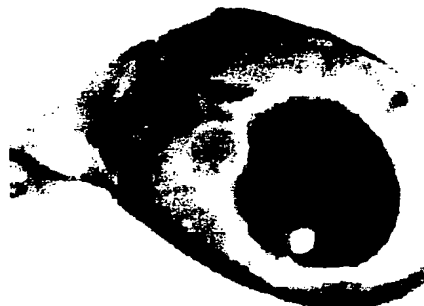
day 9 / rabbit 1 / left / nC



day 9 / rabbit 1 / right / VEGF high



day 9 / rabbit 2 / left / PMA



day 9 / rabbit 2 / left / VEGF low



day 9 / rabbit 3 / left / VEGF high



day 9 / rabbit 3 / right / PMA



day 9 / rabbit 4 / left / PMA



day 9 / rabbit 4 / right / nC

10/23



Figure 8

## BEST AVAILABLE COPY

11/23

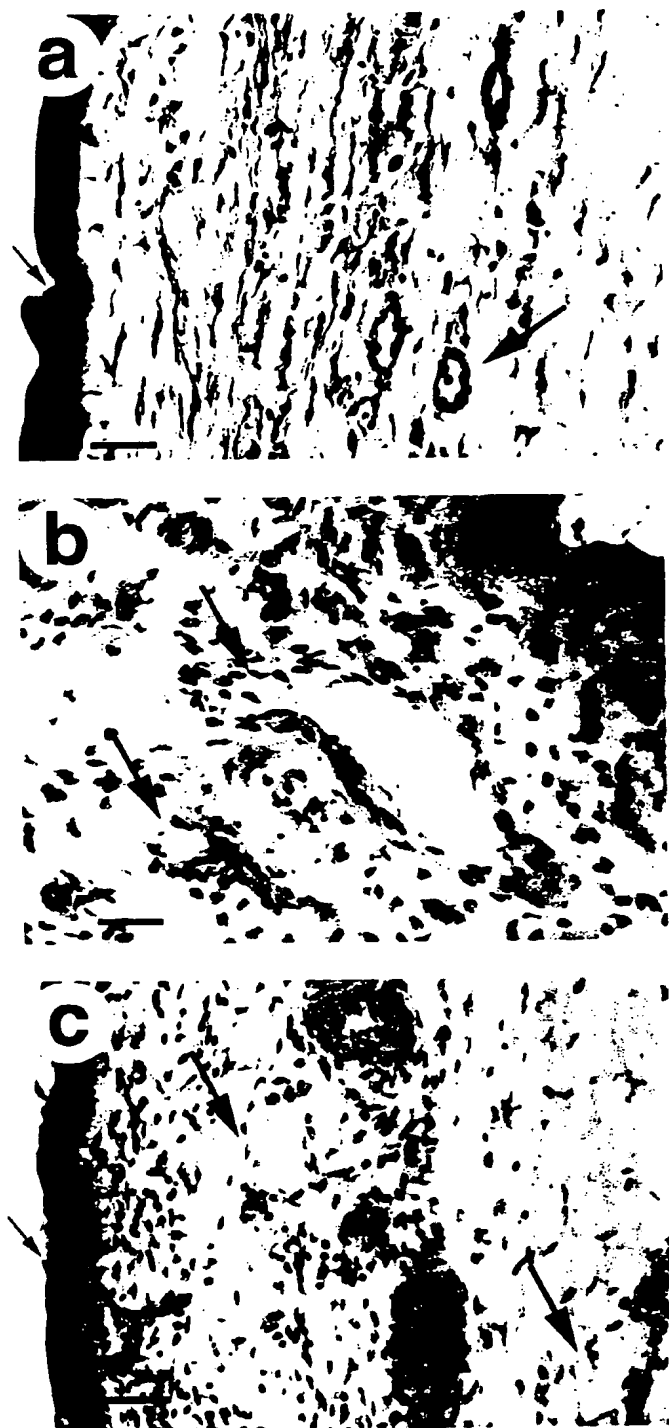


Figure 9

12/23

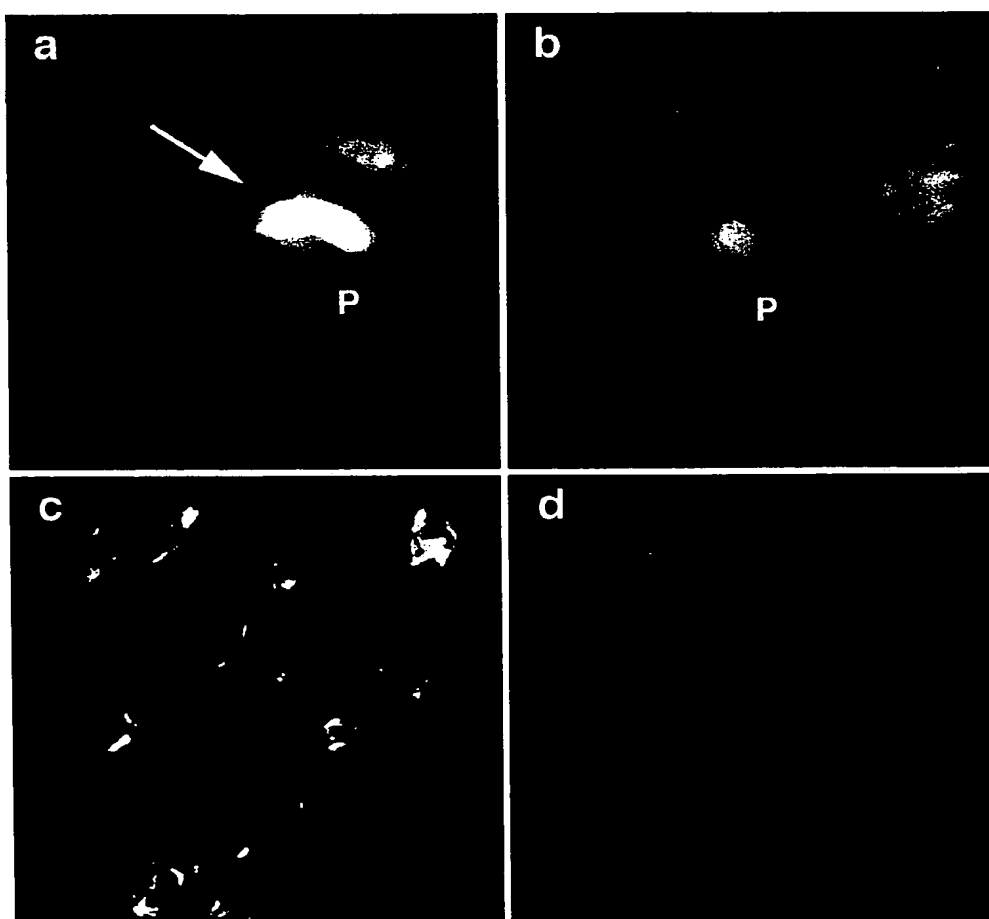


Figure 10

13/23

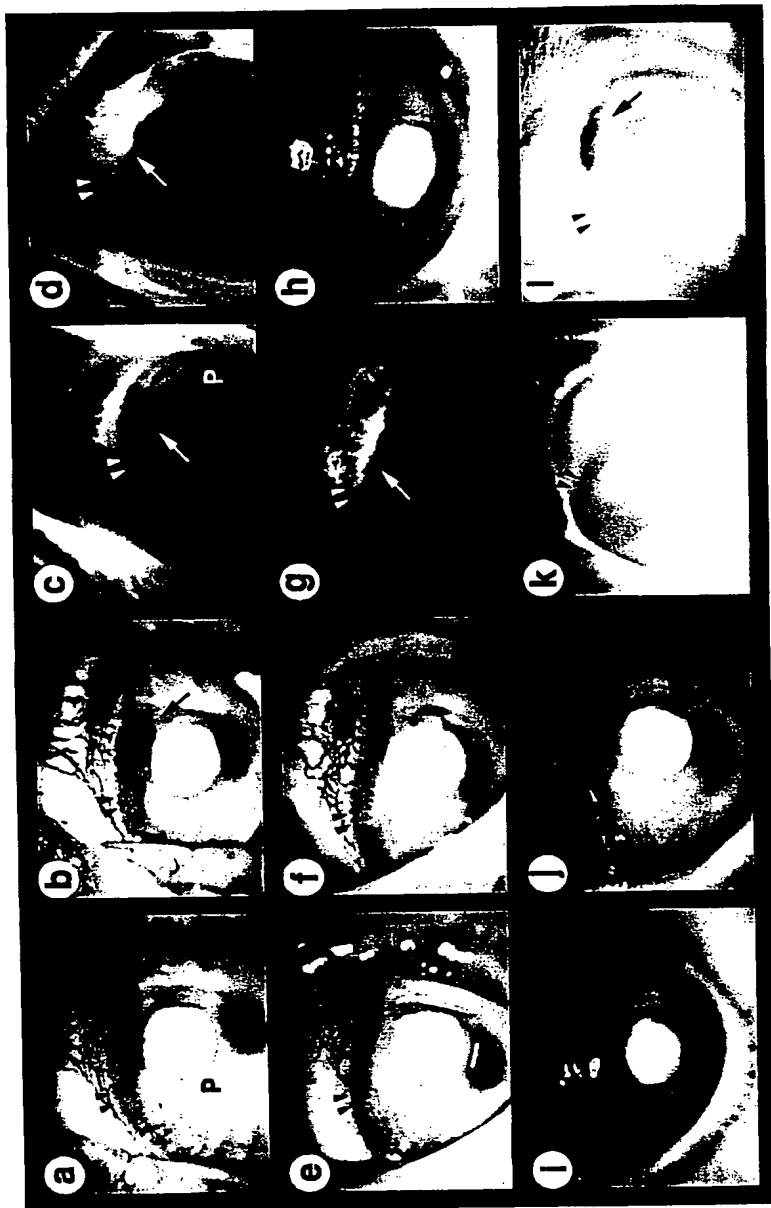


Figure 11

**BEST AVAILABLE COPY**

14/23

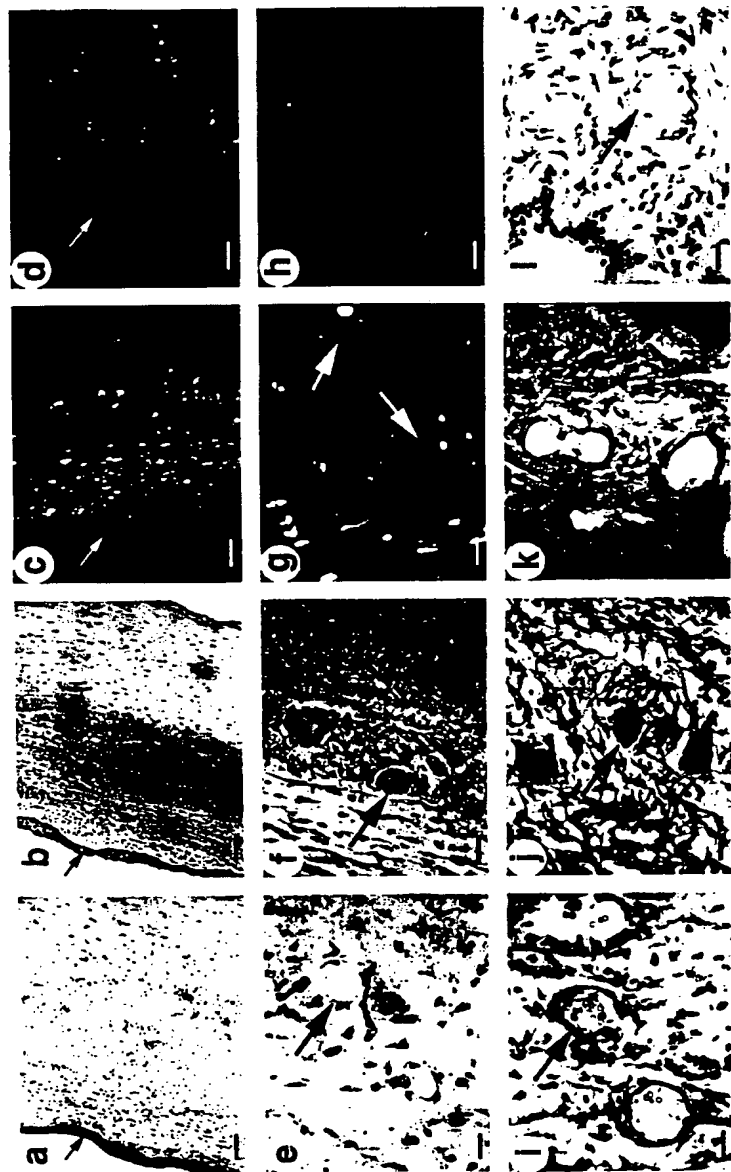
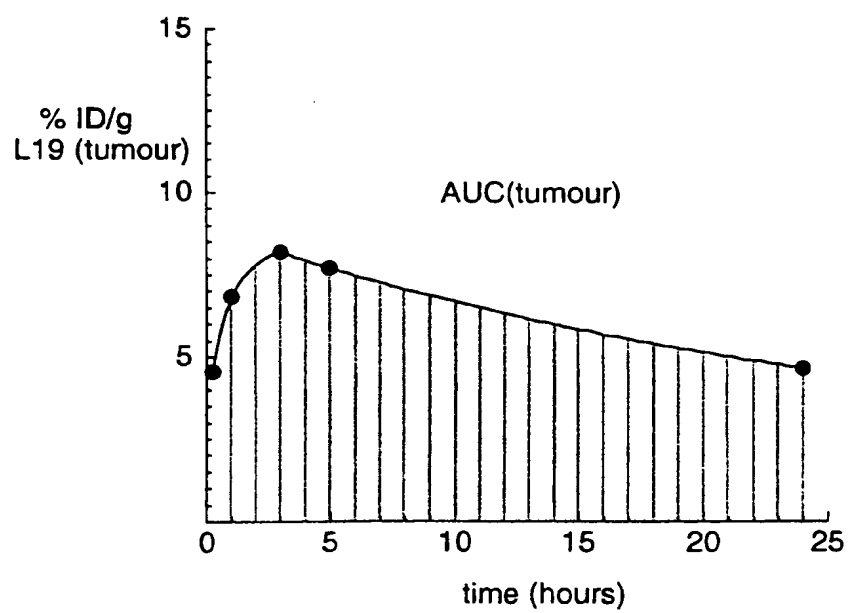
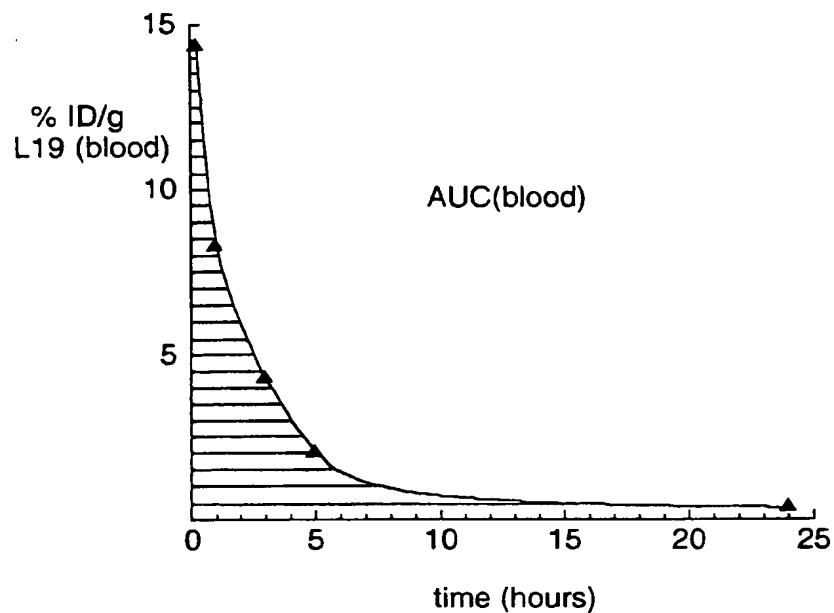
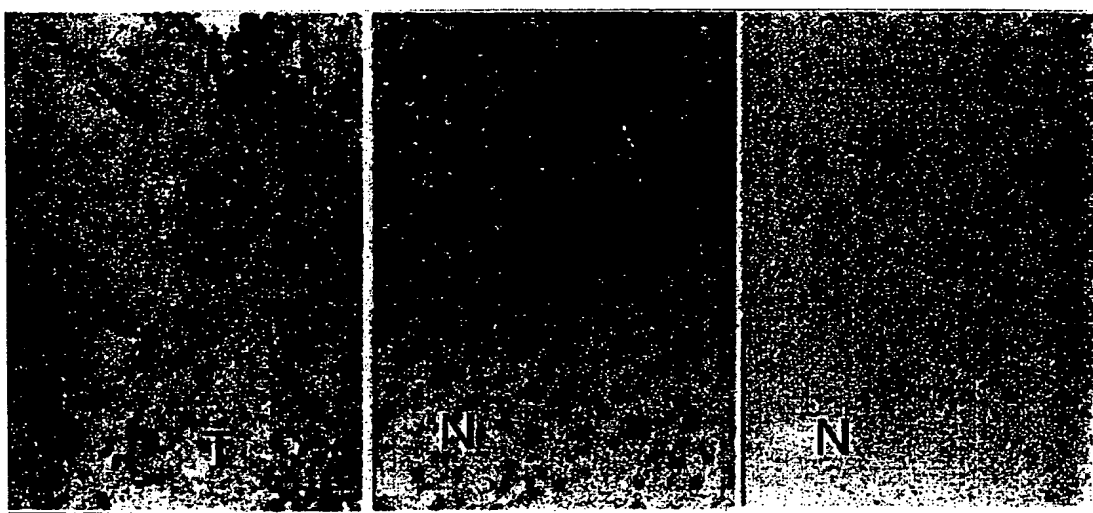


Figure 12

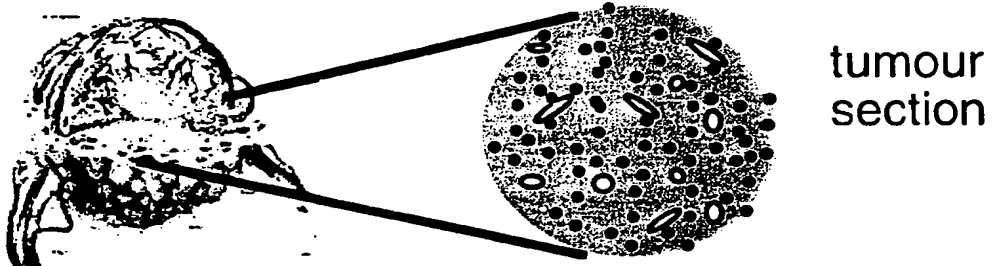
**Figure 13**

16/23

**Figure 14**



## Radioimmunotherapy with anti-angiogenesis antibodies



vessels = 0.5 - 5%  
of total tumour mass

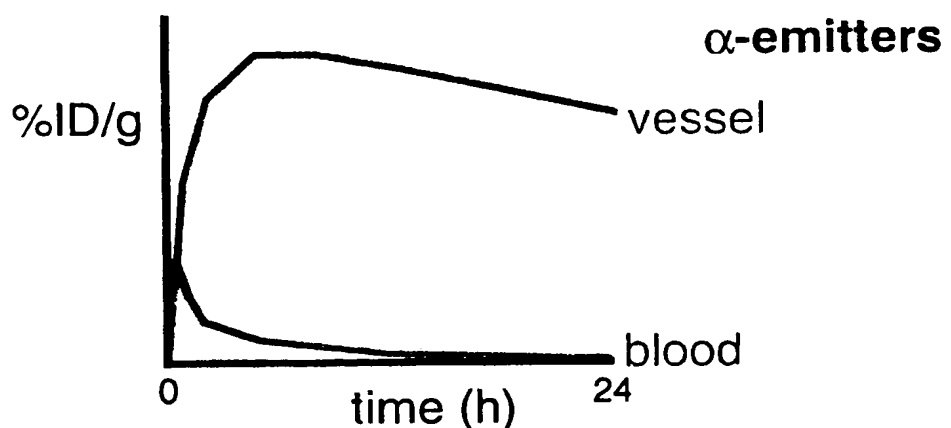
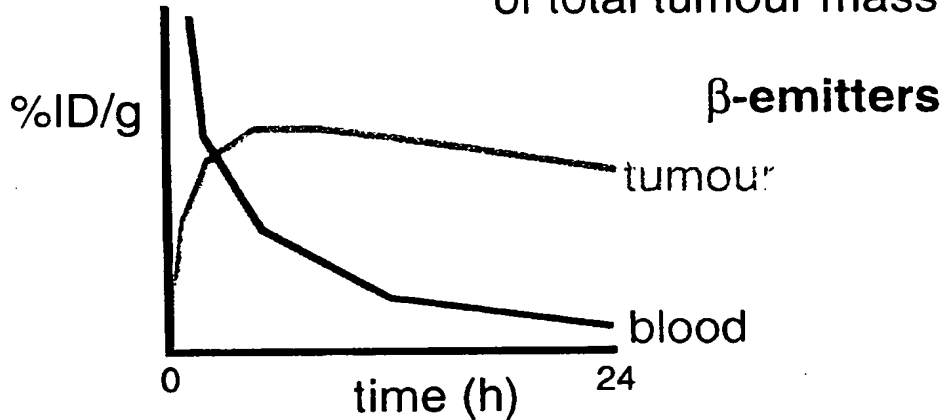


Figure 15

18/23

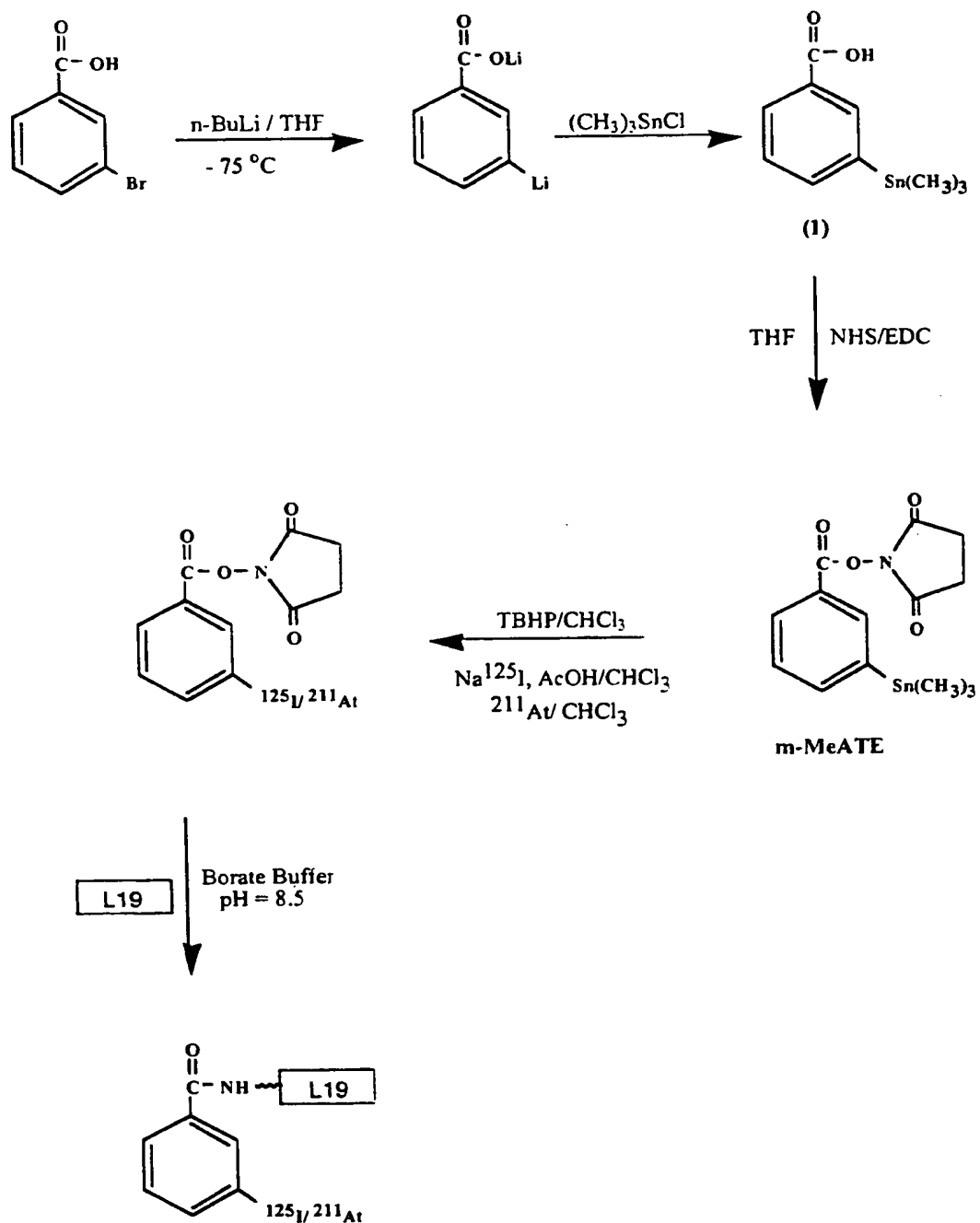
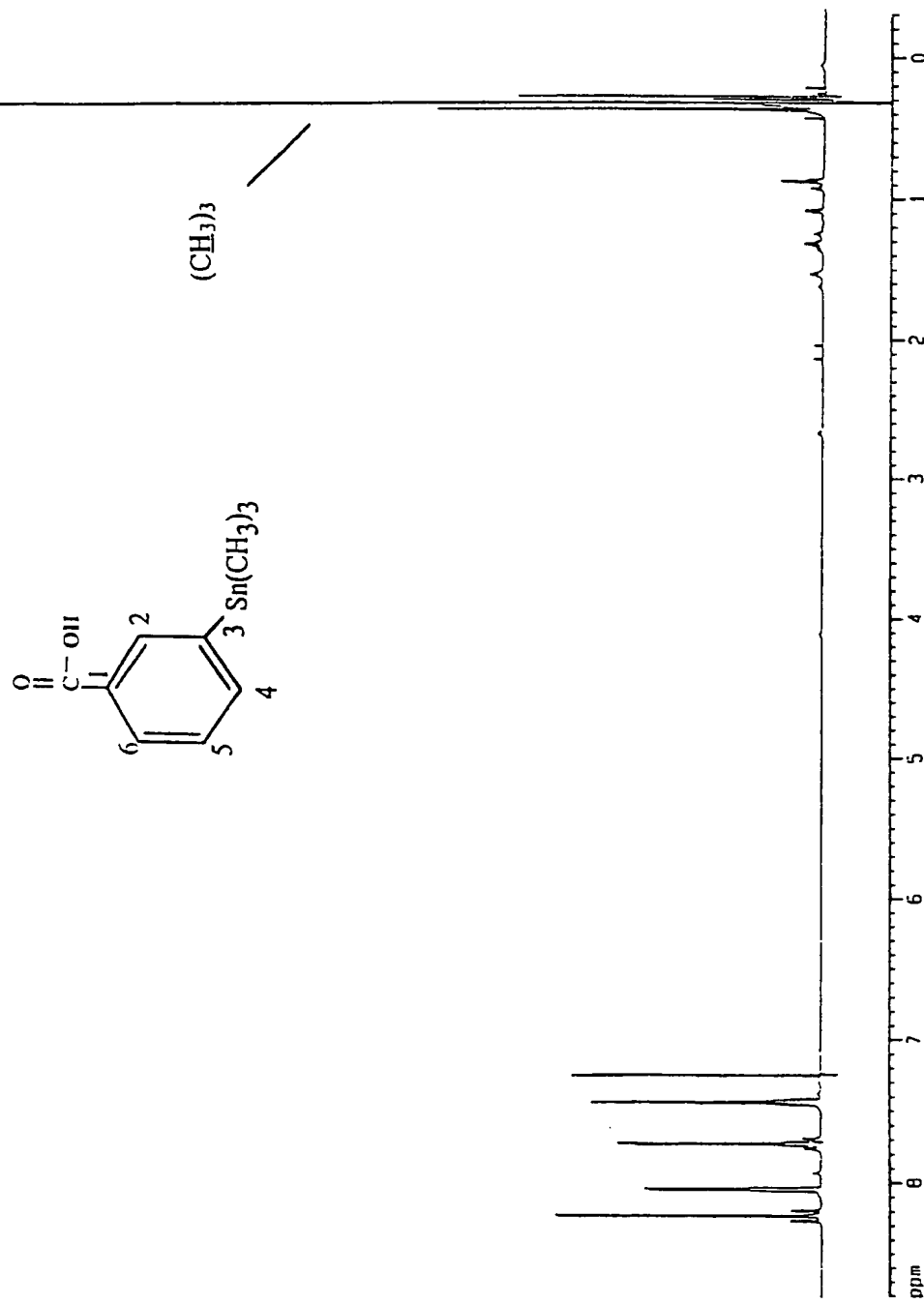


Figure 16

19/23

**Figure 17a**  
 $^1\text{H-NMR}$  spectrum of 3-(trimethylstannyl)-benzoic acid in  $\text{CDCl}_3$



19'/23

## Current Data Parameters

NAME test\_0804  
 EXPNO 1  
 PHOCNO 1

## F2 - Acquisition Parameters

Date\_ 990804  
 Time 11.19  
 INSTRUM drx600  
 PROBHD 5 mm TXI 13C  
 PULPROG zgpr.eth  
 TD 8192  
 SOLVENT CDCl3  
 NS 16  
 DS 2  
 SWH 9615.385 Hz  
 FIORES 1.173753 Hz  
 AQ 0.4260340 sec  
 RG 800  
 DW 52.000 usec  
 DE 8.00 usec  
 TE 294.0 K  
 D1 1.0000000 sec

Figure 17a'

## \*\*\*\*\* CHANNEL f1 \*\*\*\*\*

NUC1 1H  
 P1 8.00 usec  
 PL1 0.00 dB  
 PL9 120.00 dB  
 SF01 600.1328114 MHz

## \*\*\*\*\* GRADIENT CHANNEL \*\*\*\*\*

GPNAME sine.32  
 GPX1 0.00 x  
 GPY1 0.00 x  
 GPZ1 50.00 x  
 P21 1000.00 usec

## F2 - Processing parameters

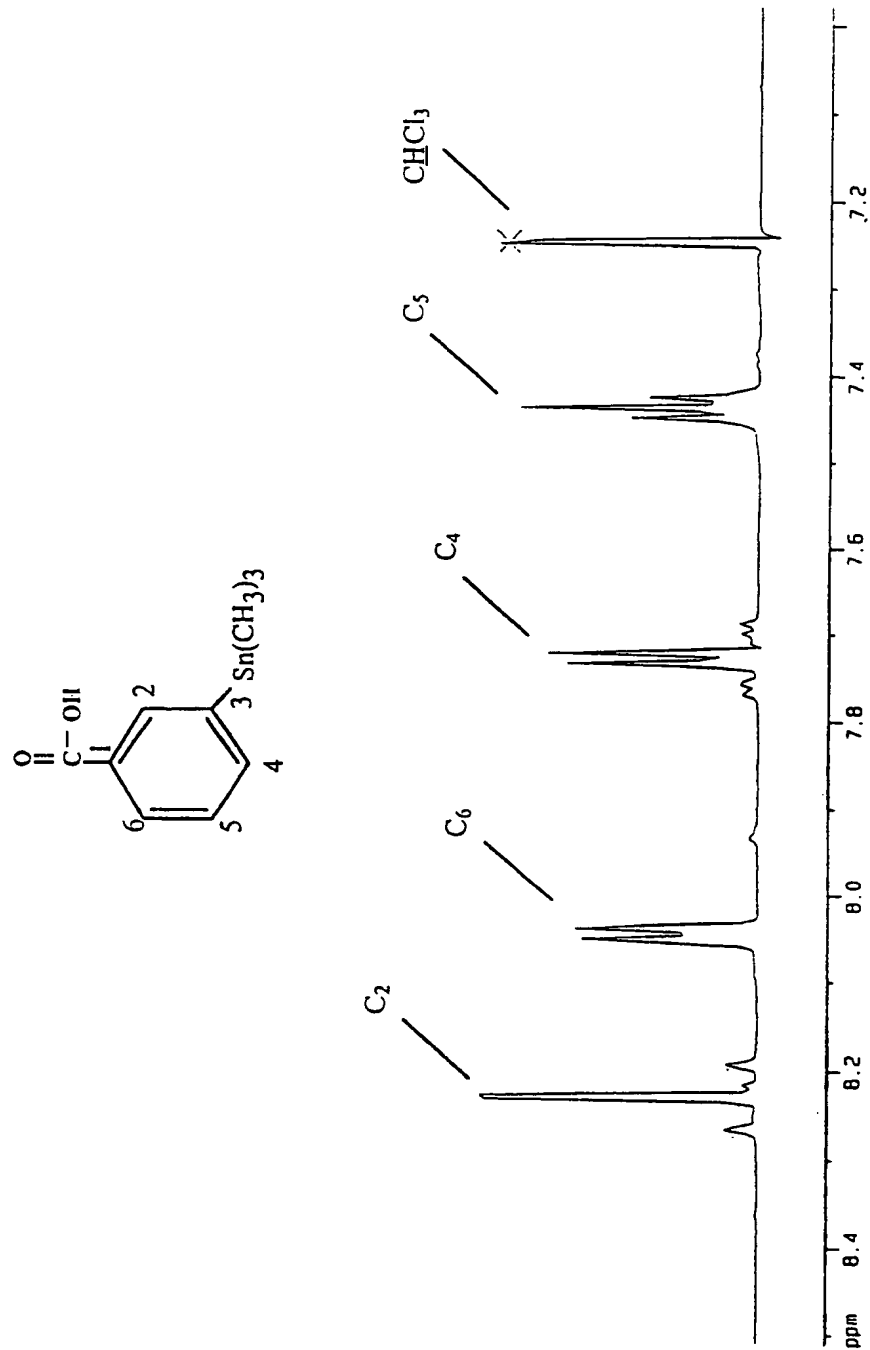
SI 4096  
 SF 600.1300239 MHz  
 WDW QSINE  
 SSB 3  
 LB 0.00 Hz  
 GB 0  
 PC 1.00

## 1D NMR plot parameters

CX 20.00 cm  
 F1P 8.811 ppm  
 F1 5287.97 Hz  
 F2P -0.341 ppm  
 F2 -204.86 Hz  
 PPMCM 0.45764 ppm/cm  
 HZCM 274.64160 Hz/cm

20/23

**Figure 17b**  
<sup>1</sup>H-NMR spectrum of 3-(trimethylstannyl)-benzoic acid in CDCl<sub>3</sub>



20/23

```

Current Data Parameters
NAME          test_0804
EXPNO         1
PROCNO        1

F2 - Acquisition Parameters
Date_        990804
Time_        11.19
INSTRUM      drx600
PROBHD      5 mm TXI 13C
PULPROG      zgpr.eth
TD           8192
SOLVENT      C6C13
NS            16
DS            2
SWH          9615.385 Hz
FIDRES       1.173753 Hz
AQ           0.4260340 sec
RG           800
DW           52.000 usec
DE           8.00 usec
TE           294.0 K
D1           1.0000000 sec

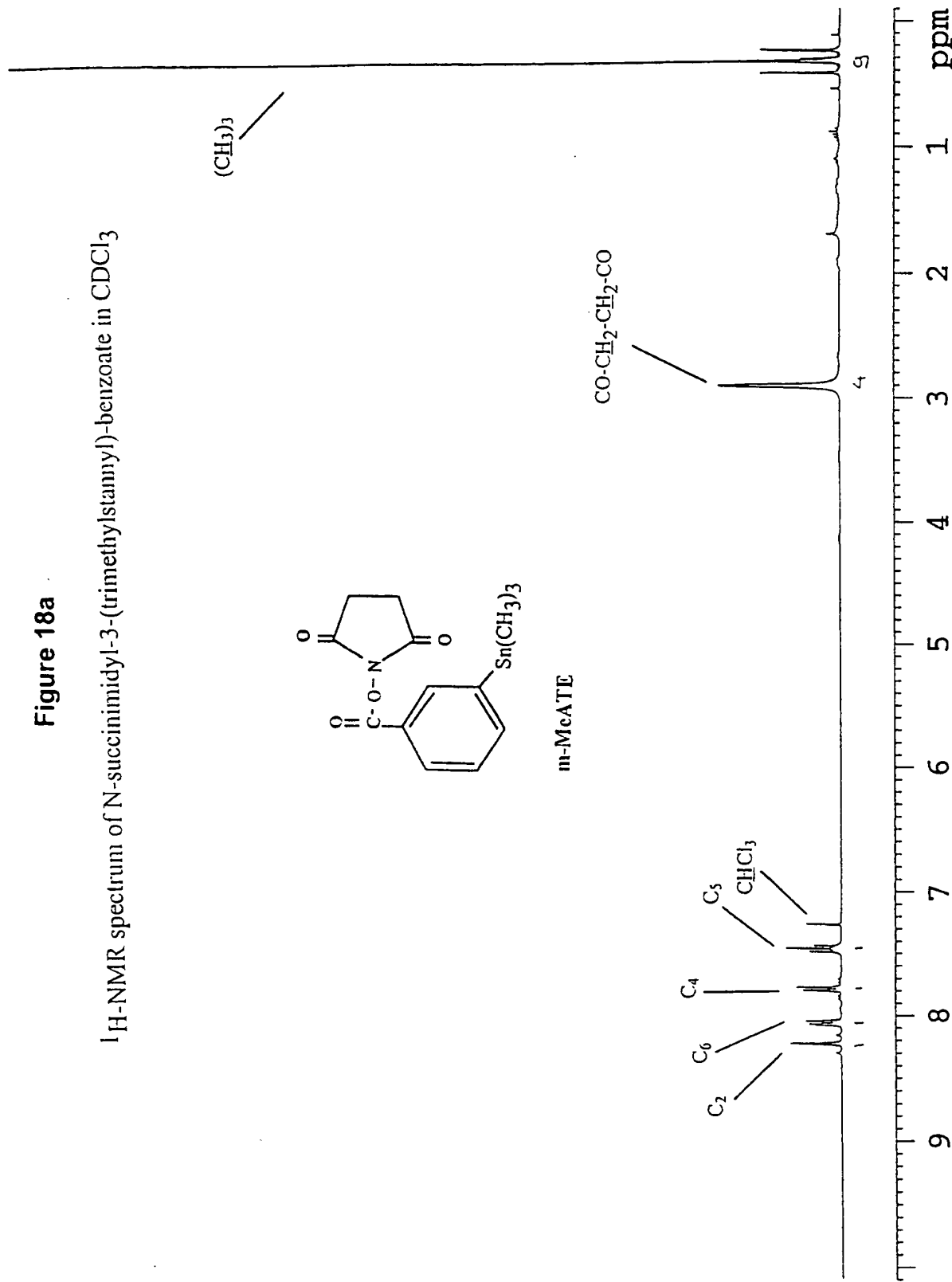
Figure 17b
***** CHANNEL f1 *****
NUC1          1H
P1            8.00 usec
PL1           0.00 dB
PL9           120.00 dB
SF01          600.1328114 MHz

***** GRADIENT CHANNEL *****
GPNAM1        sine.32
GPX1           0.00 x
GPY1           0.00 x
GPZ1           50.00 x
P21           1000.00 usec

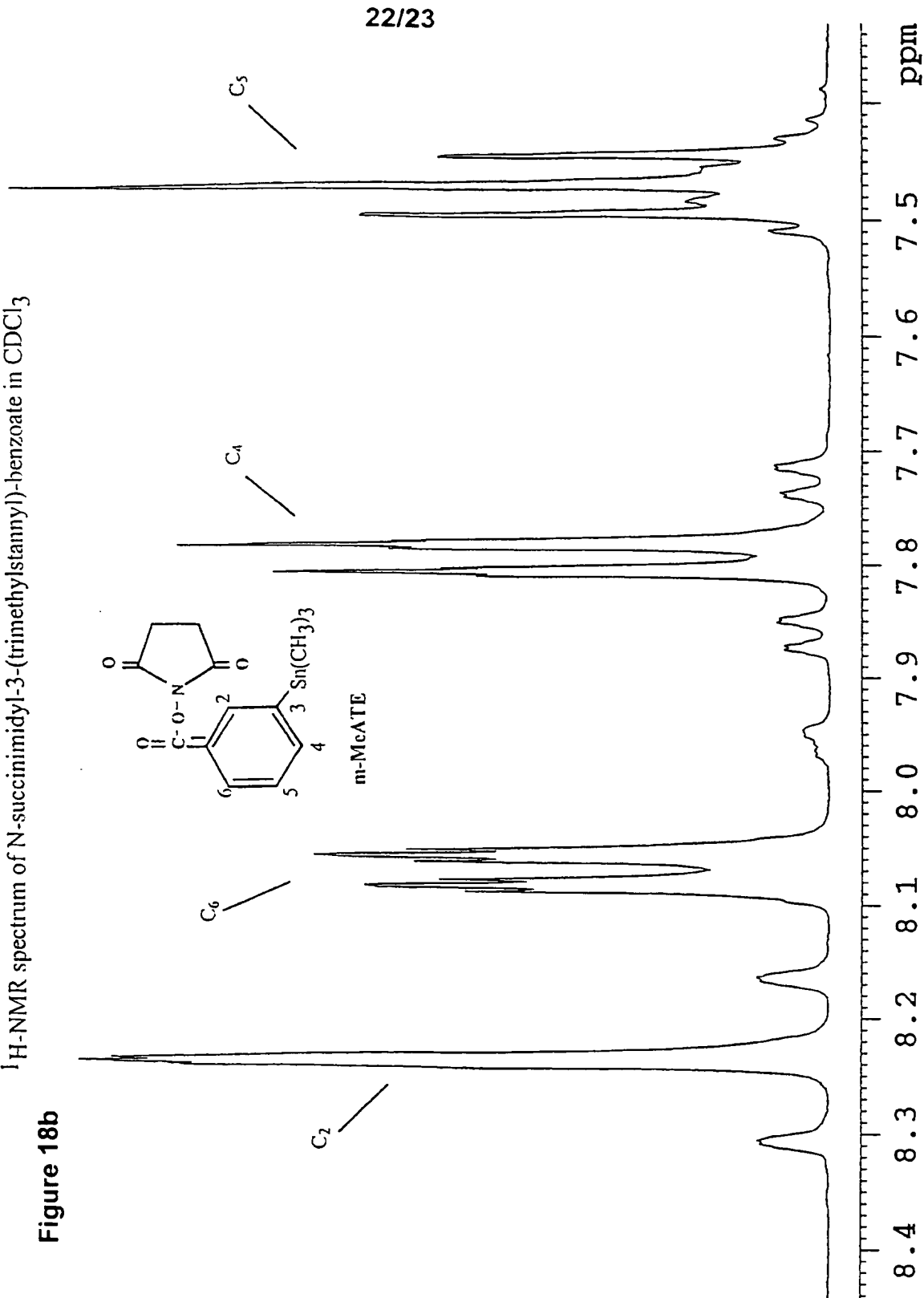
F2 - Processing parameters
SI            4096
SF           600.1300239 MHz
WMW          OSINE
SSB            3
LB            0.00 Hz
GB            0
PC            1.00

1D NMR plot parameters
CX           20.00 cm
F1P          8.513 ppm
F1           5108.78 Hz
F2P          6.977 ppm
F2           4187.17 Hz
PPNCHM       0.07678 ppm/cm
HZCH        46.08082 Hz/cm

```

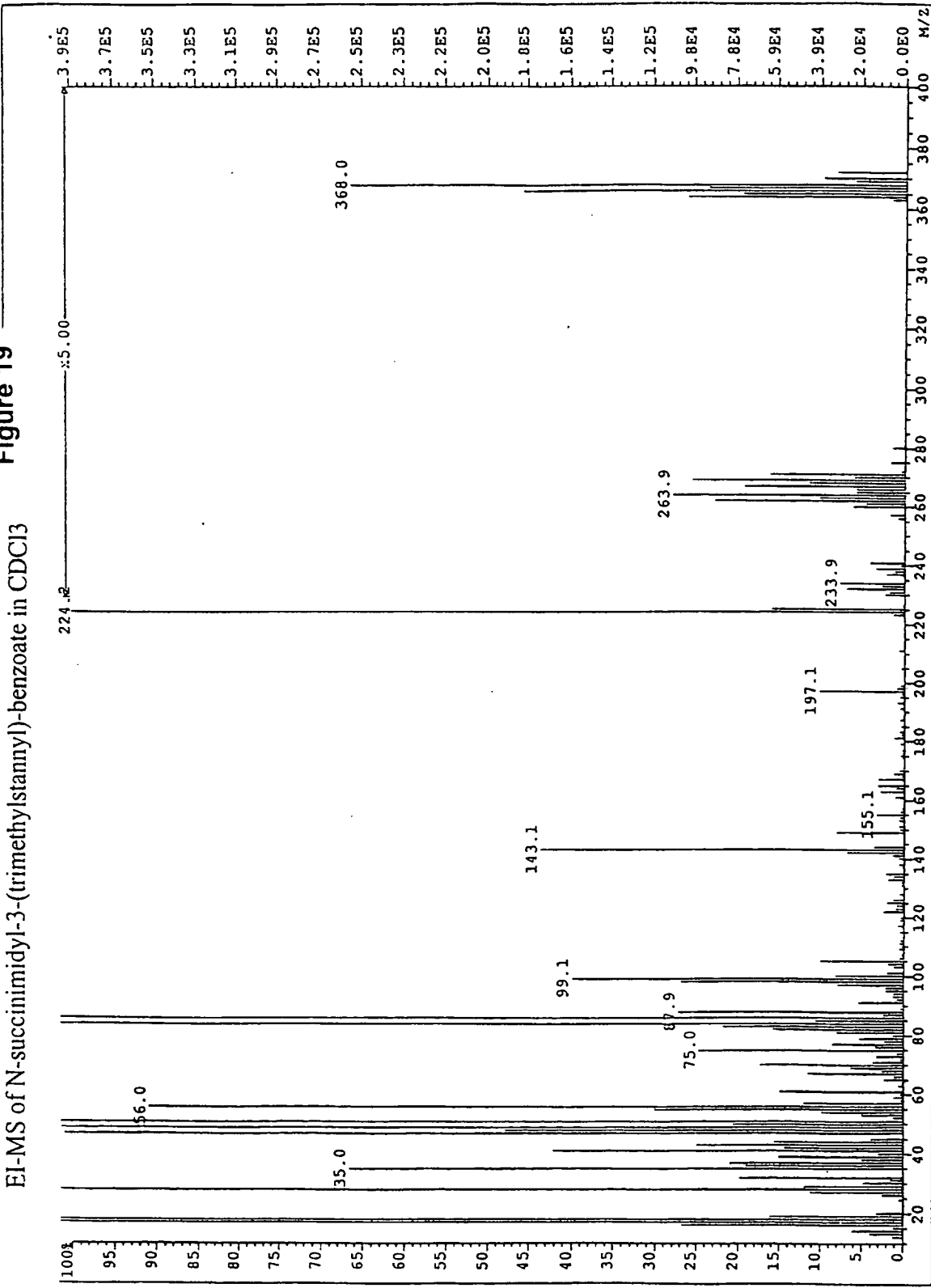


**Figure 18b**  
<sup>1</sup>H-NMR spectrum of N-succinimidyl-3-(trimethylstanny)-benzoate in CDCl<sub>3</sub>



23/23

Figure 19

EI-MS of N-succinimidyl-3-(trimethylsilyanyl)-benzoate in CDCl<sub>3</sub>

SUBSTITUTE SHEET (RULE 26)

## 1

## SEQUENCE LISTING

<110> Eidgenoessische Technische Hochschule Zuerich

<120> Specific binding molecules for scintigraphy, conjugates containing them and therapeutic method for treatment of angiogenesis

<130> 1900PTWO2

<140>  
<141>

<150> US 09/512,082  
<151> 2000-02-24

<160> 21

<170> PatentIn Ver. 2.0

<210> 1  
<211> 24  
<212> DNA  
<213> Artificial Sequence  
<220>  
<223> Description of Artificial Sequence: PCR primer:  
LMBlbis

<400> 1  
gcggcccaaggc cggccatggc cgag 24

<210> 2  
<211> 54  
<212> DNA  
<213> Artificial Sequence  
<220>  
<223> Description of Artificial Sequence: PCR primer:  
DP47CDR1for

<400> 2  
gagcctggcg gaccaggctc atmnnnnnnnn ngttaaaggtaaatccagag gctg 54

<210> 3  
<211> 23  
<212> DNA  
<213> Artificial Sequence  
<220>  
<223> Description of Artificial Sequence: PCR primer:  
DP47CDR1back

<400> 3  
atgagctggg tccggcaggc tcc 23

<210> 4  
<211> 60  
<212> DNA  
<213> Artificial Sequence  
<220>  
<223> Description of Artificial Sequence: PCR primer:  
DP47CDR2for

<400> 4  
gtctgcgtatatgtggtag cmnnactacc mnnaatmnnt gagacccact ccagcccc 60

<210> 5  
<211> 24  
<212> DNA  
<213> Artificial Sequence  
<220>  
<223> Description of Artificial Sequence: PCR primer:  
DP47CDR2back

<400> 5  
acatactacg cagactccgt gaag 24

<210> 6  
<211> 53  
<212> DNA  
<213> Artificial Sequence  
<220>  
<223> Description of Artificial Sequence: PCR primer:  
JforNot

<400> 6  
tcattctcga cttgcggccg ctttgatttc caccttggtc cttggccga acg 53

<210> 7  
<211> 47  
<212> DNA  
<213> Artificial Sequence  
<220>  
<223> Description of Artificial Sequence: PCR primer:  
DPKCDR1for

<400> 7  
gtttctgtgt gtaccaggct aamnngctgc tgctaacact ctgactg 47

<210> 8  
<211> 23  
<212> DNA  
<213> Artificial Sequence  
<220>  
<223> Description of Artificial Sequence: PCR primer:  
DPKCDR1back

<400> 8  
ttagcctggtaaccaggagaa acc 23

<210> 9  
<211> 46  
<212> DNA  
<213> Artificial Sequence  
<220>  
<223> Description of Artificial Sequence: PCR primer:  
DPKCDR2for

<400> 9  
gccagtggcc ctgctggatg cmnnatagat gaggagcctg ggagcc 46

<210> 10  
<211> 21  
<212> DNA  
<213> Artificial Sequence

<220>  
<223> Description of Artificial Sequence: PCR primer:  
DPKCDR2back

<400> 10  
gcatccagca gggccactgg c 21

<210> 11  
<211> 45  
<212> DNA  
<213> Artificial Sequence  
<220>  
<223> Description of Artificial Sequence: PCR primer:  
DP47baNco

<400> 11  
gcggcccccagc atgccatggc cgaggtgcag ctgttggagt ctggg 45

<210> 12  
<211> 55  
<212> DNA  
<213> Artificial Sequence  
<220>  
<223> Description of Artificial Sequence: PCR primer:  
CDR3for

<400> 12  
ggttccctgg ccccagtagt caaamnnnnn mnnnnnnnttc gcacagtaat atacg 55

<210> 13  
<211> 24  
<212> DNA  
<213> Artificial Sequence  
<220>  
<223> Description of Artificial Sequence: PCR primer:  
VHpullth

<400> 13  
gcggcccccagc atgccatggc cgag 24

<210> 14  
<211> 66  
<212> DNA  
<213> Artificial Sequence  
<220>  
<223> Description of Artificial Sequence: PCR primer:  
Jassm

<400> 14  
cccgcttaccg ccactggacc catcgccact cgagacggtg accagggttc cctggcccca 60  
gtatgc 66

<210> 15  
<211> 62  
<212> DNA  
<213> Artificial Sequence  
<220>  
<223> Description of Artificial Sequence: PCR primer:  
DPK22assm

<400> 15  
gatgggtcca gtggcggtag cgggggcgcg tcgactggcg aaattgtgtt gacgcagtct 60  
cc 62

```

<210> 16
<211> 63
<212> DNA
<213> Artificial Sequence
<220>
<223> Description of Artificial Sequence: PCR primer:
      DPK3for

<400> 16
caccttggtc ccttggccga acgtmnnncgg mnnmnnnaccm nnctgctgac agtaatacac 60
tgc                                         63

<210> 17
<211> 56
<212> DNA
<213> Artificial Sequence
<220>
<223> Description of Artificial Sequence: PCR primer:
      Jfornot

<400> 17
gagtcattct cgacttgcgg ccgcattgtat ttccacatttgc gtcccttggc cgaacg      56

<210> 18
<211> 24
<212> DNA
<213> Artificial Sequence
<220>
<223> Description of Artificial Sequence: PCR primer:
      VIpullth

<400> 18
gatgggtcca gtggcggttag cggg                                         24

<210> 19
<211> 116
<212> PRT
<213> VH antibody specific for ED-B domain of fibronectin

<400> 19
Glu Val Gln Leu Leu Glu Ser Gly Gly Gly Leu Val Gln Pro Gly Gly
  1           5           10          15

Ser Leu Arg Leu Ser Cys Ala Ala Ser Gly Phe Thr Phe Ser Ser Phe
  20          25          30

Ser Met Ser Trp Val Arg Gln Ala Pro Gly Lys Gly Leu Glu Trp Val
  35          40          45

Ser Ser Ile Ser Gly Ser Ser Gly Thr Thr Tyr Tyr Ala Asp Ser Val
  50          55          60

Lys Gly Arg Phe Thr Ile Ser Arg Asp Asn Ser Lys Asn Thr Leu Tyr
  65          70          75          80

Leu Gln Met Asn Ser Leu Arg Ala Glu Asp Thr Ala Val Tyr Tyr Cys
  85          90          95

Ala Lys Pro Phe Pro Tyr Phe Asp Tyr Trp Gly Gln Gly Thr Leu Val
  100         105         110

```

Thr Val Ser Ser  
115

<210> 20  
<211> 14  
<212> PRT  
<213> Artificial Sequence  
<220>  
<223> Description of Artificial Sequence: antibody linker

<400> 20  
Gly Asp Gly Ser Ser Gly Gly Ser Gly Ala Ser Thr Gly  
1 5 10

<210> 21  
<211> 108  
<212> PRT  
<213> VL antibody specific for ED-B domain of fibronectin

<400> 21  
Glu Ile Val Leu Thr Gln Ser Pro Gly Thr Leu Ser Leu Ser Pro Gly  
1 5 10 15

Glu Arg Ala Thr Leu Ser Cys Arg Ala Ser Gln Ser Val Ser Ser Ser  
20 25 30

Tyr Leu Ala Trp Tyr Gln Gln Lys Pro Gly Gln Ala Pro Arg Leu Leu  
35 40 45

Ile Tyr Tyr Ala Ser Ser Arg Ala Thr Gly Ile Pro Asp Arg Phe Ser  
50 55 60

Gly Ser Gly Ser Gly Thr Asp Phe Thr Leu Thr Ile Ser Arg Leu Glu  
65 70 75 80

Pro Glu Asp Phe Ala Val Tyr Tyr Cys Gln Gln Thr Gly Arg Ile Pro  
85 90 95

Pro Thr Phe Gly Gln Gly Thr Lys Val Glu Ile Lys  
100 105

# INTERNATIONAL SEARCH REPORT

International Application No  
PCT/EP 01/02062

**A. CLASSIFICATION OF SUBJECT MATTER**

IPC 7	C07K16/18	A61K51/10	G01N33/53	G01N33/574	G01N33/577
	C07C63/06	A61P35/00			

According to International Patent Classification (IPC) or to both national classification and IPC

**B. FIELDS SEARCHED**

Minimum documentation searched (classification system followed by classification symbols)

IPC 7 C07K

Documentation searched other than minimum documentation to the extent that such documents are included in the fields searched

Electronic data base consulted during the international search (name of data base and, where practical, search terms used)

BIOSIS, EMBASE, CHEM ABS Data, WPI Data, PAJ, EPO-Internal

**C. DOCUMENTS CONSIDERED TO BE RELEVANT**

Category	Citation of document, with indication, where appropriate, of the relevant passages	Relevant to claim No.
X	WO 99 58570 A (EIDGENÖSSISCHE TECHNISCHE HOCHSCHULE ZÜRICH) 18 November 1999 (1999-11-18) the whole document	1-24, 29-31
Y	----	25-28, 32-35

Further documents are listed in the continuation of box C.

Patent family members are listed in annex.

\* Special categories of cited documents :

- \*A\* document defining the general state of the art which is not considered to be of particular relevance
- \*E\* earlier document but published on or after the international filing date
- \*L\* document which may throw doubts on priority claim(s) or which is cited to establish the publication date of another citation or other special reason (as specified)
- \*O\* document referring to an oral disclosure, use, exhibition or other means
- \*P\* document published prior to the international filing date but later than the priority date claimed

\*T\* later document published after the international filing date or priority date and not in conflict with the application but cited to understand the principle or theory underlying the invention

\*X\* document of particular relevance; the claimed invention cannot be considered novel or cannot be considered to involve an inventive step when the document is taken alone

\*Y\* document of particular relevance; the claimed invention cannot be considered to involve an inventive step when the document is combined with one or more other such documents, such combination being obvious to a person skilled in the art.

\*&\* document member of the same patent family

Date of the actual completion of the international search

13 July 2001

Date of mailing of the international search report

27/07/2001

Name and mailing address of the ISA

European Patent Office, P.B. 5818 Patentlaan 2  
NL - 2280 HV Rijswijk  
Tel. (+31-70) 340-2040, Tx. 31 651 epo nl.  
Fax: (+31-70) 340-3016

Authorized officer

Nooij, F

# INTERNATIONAL SEARCH REPORT

International Application No

PCT/EP 01/02062

C.(Continuation) DOCUMENTS CONSIDERED TO BE RELEVANT

Category	Citation of document, with indication, where appropriate, of the relevant passages	Relevant to claim No.
Y	<p>M. ZALUTSKY ET AL.: "Labeling monoclonal antibodies and F(ab')2 fragments with the alpha-particle-emitting nuclide astatine-211: preservation of immunoreactivity and in vivo localization." PROCEEDINGS OF THE NATIONAL ACADEMY OF SCIENCES OF THE U.S.A., vol. 86, no. 18, September 1989 (1989-09), pages 7149-7153, XP002172060 Washington, DC, USA abstract</p> <p>---</p> <p>S. LINDEGREN ET AL.: "Chloramine-T in high-specific-activity radioiodination of antibodies using N-succinimidyl-3-(trimethylstannyl)benzoate as an intermediate." NUCLEAR MEDICINE AND BIOLOGY, vol. 25, no. 7, October 1998 (1998-10), pages 659-665, XP004149436 Oxford, GB abstract</p> <p>---</p> <p>WO 97 45544 A (MEDICAL RESEARCH COUNCIL ET AL.) 4 December 1997 (1997-12-04) cited in the application the whole document</p> <p>---</p> <p>M. BIRCHLER ET AL.: "Selective targeting and photocoagulation of ocular angiogenesis mediated by a phage-derived human antibody fragment." NATURE BIOTECHNOLOGY, vol. 17, no. 10, October 1999 (1999-10), pages 984-988, XP002172061 New York, NY, USA the whole document</p> <p>---</p> <p>A. PINI ET AL.: "Design and use of a phage display library." THE JOURNAL OF BIOLOGICAL CHEMISTRY, vol. 273, no. 34, 21 August 1998 (1998-08-21), pages 21769-21776, XP002124781 Baltimore, MD, USA the whole document</p> <p>---</p> <p style="text-align: right;">-/--</p>	25-28, 32-34
Y		35
X		1,3-5, 14,18,19
X		1-11, 14-24, 29-31
X		1-11

# INTERNATIONAL SEARCH REPORT

Int. Application No

PCT/EP 01/02062

## C.(Continuation) DOCUMENTS CONSIDERED TO BE RELEVANT

Category	Citation of document, with indication, where appropriate, of the relevant passages	Relevant to claim No.
X	<p>F. VITI ET AL.: "Increased binding affinity and valence of recombinant antibody fragments lead to improved targeting of tumoral angiogenesis."</p> <p>CANCER RESEARCH,</p> <p>vol. 59, no. 2, 15 January 1999 (1999-01-15), pages 347-352, XP002124782</p> <p>Philadelphia, PA, USA</p> <p>the whole document</p> <p>---</p>	1-19
X	<p>L.TARLI ET AL.: "A high-affinity human antibody that targets tumoral blood vessels."</p> <p>BLOOD,</p> <p>vol. 94, no. 1, 1 July 1999 (1999-07-01), pages 192-198, XP002124784</p> <p>New York, NY, USA</p> <p>the whole document</p> <p>-----</p>	1-19

**FURTHER INFORMATION CONTINUED FROM PCT/ISA/ 210**

This International Searching Authority found multiple (groups of) inventions in this international application, as follows:

1. Claims: 1-34

High affinity antibody specific for an epitope of the ED-B domain of fibronectin, immunoconjugates thereof and their diagnostic and therapeutic use.

2. Claim : 35

3-(trimethylstanny1)benzoic acid

**FURTHER INFORMATION CONTINUED FROM PCT/ISA/ 210**

Continuation of Box I.1

Although claims 14, 17 and 19 (all partially, as far as an in vivo method of diagnosis is concerned) and 15 and 16 (both completely) are directed to a diagnostic method practised on the human/animal body, and although claims 14, 17 and 19 (all partially, as far as an in vivo method of treatment is concerned) and claims 29-34 (all completely) are directed to a method of treatment of the human/animal body, the search has been carried out and based on the alleged effects of the compound/composition.

# INTERNATIONAL SEARCH REPORT

## Information on patent family members

International Application No

PCT/EP 01/02062

Patent document cited in search report	Publication date	Patent family member(s)			Publication date
WO 9958570	A 18-11-1999	AU	4039899	A	29-11-1999
		BR	9910394	A	09-01-2001
		EP	1084145	A	21-03-2001
		NO	20005694	A	10-01-2001
-----	-----	-----	-----	-----	-----
WO 9745544	A 04-12-1997	AU	729081	B	25-01-2001
		AU	2910197	A	05-01-1998
		BG	102950	A	31-08-1999
		BR	9709350	A	04-01-2000
		CA	2256308	A	04-12-1997
		CN	1219968	A	16-06-1999
		CZ	9803815	A	17-03-1999
		EP	0906426	A	07-04-1999
		JP	2000511416	T	05-09-2000
		NO	985459	A	22-01-1999
		PL	330075	A	26-04-1999
		SK	161298	A	12-07-1999
		TR	9802416	T	22-02-1999
-----	-----	-----	-----	-----	-----